

Functional Group Bridge for Simultaneous Regression and Support Estimation

Zhengjia Wang

Department of Statistics, Rice University

John Magnotti

Department of Neurosurgery and Core for Advanced MRI

Baylor College of Medicine

Michael S. Beauchamp

Department of Neurosurgery and Core for Advanced MRI

Baylor College of Medicine

Meng Li

Department of Statistics, Rice University

Abstract

There is a wide variety of applications where the unknown nonparametric functions are locally sparse, and the support of a function as well as the function itself is of primary interest. In the function-on-scalar setting, while there has been a rich literature on function estimation, the study of recovering the function support is limited. In this article, we consider the function-on-scalar mixed effect model and propose a weighted group bridge approach for simultaneous function estimation and support recovery, while accounting for heterogeneity present in functional data. We use B-splines to transform sparsity of functions to its sparse vector counterpart of increasing dimension, and propose a fast non-convex optimization algorithm for estimation. We show that the estimated coefficient functions are rate optimal in the minimax sense under the L_2 norm and resemble a phase transition phenomenon. For support estimation, we derive a convergence rate under the L_∞ norm that leads to a sparsistency property under δ -sparsity, and provide a simple sufficient regularity condition under which a strict sparsistency property is established. An adjusted extended Bayesian information criterion is proposed for parameter tuning. The developed method is illustrated through simulation and an application to a novel intracranial electroencephalography (iEEG) dataset.

Keywords: Function-on-scalar regression, iEEG, minimax rate, non-convex optimization, sparsistency, supremum norm

1 Introduction

Functional data analysis (FDA) is routinely encountered in modern applications due to the rapid advancement of new techniques to collect high-resolution data that can be viewed as curves; see Ferraty and Vieu (2006); Morris (2015); Ramsay and Silverman (2005); Wang et al. (2016) for a comprehensive treatment. An overwhelming focus has been on nonparametric estimation of the underlying function on either the Euclidean space under various designs or manifold. However, shape constraints arise naturally in many modern applications. In the nonparametric literature, various shapes including convexity, monotonicity, uni-modality, (log-)concavity have been incorporated into estimating the underlying surface; for example, see Abraham and Khadraoui (2015); Gunn and Dunson (2005); Holmes and Heard (2003); Meyer (2008); Ramsay (1998); Shively et al. (2009, 2011). Local sparsity, contrasted to *global sparsity* that refers to a zero function, is a crucial characteristic for a nonparametric method to be interpretable in a variety of applications, and the estimation of the support as well as the function itself is of primary interest. The goal of this article is to develop a flexible method with theoretical guarantees for simultaneously estimating and recovering the support of locally sparse functions.

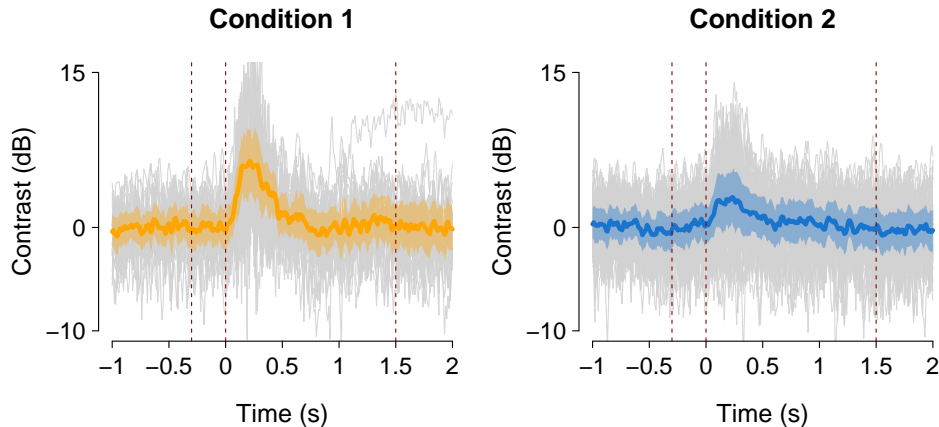


Figure 1: The data are obtained by decomposing the measured voltage signal into frequency space, converting to Decibel unit, calibrated to baseline (from -1 to -0.3 seconds), and then taking the average power in the 70-150Hz range. Each individual grey line is one trial. Bold solid lines are mean responses to different condition types. The ribbon around the mean is a pointwise 95% confidence interval.

Our motivation stems from neuroscientific studies using human intracranial electroencephalography (iEEG) data. Unlike traditional fMRI or EEG techniques, iEEG is an emerging method for invasive measurement of human brain activity. It provides excellent temporal and spatial resolution, along with high signal-to-noise ratios. With recordings directly from neurons firing and sampling rates at over thousand Hertz, the collected brain signals enable neuroscientists to study clear gamma and high-gamma oscillations that non-invasive methods can hardly compete with (Lachaux et al., 2012). In our motivating data, multi-phase experiments are designed to help understand how brain handles auditory and visual stimulus, where the contrast of brain activities is expected to be locally sparse (zero at certain period

of time) and estimation of the coefficient function as well as detection of the non-sparse region is of substantial interest to neuroscientists. For example, Figure 1 shows example data from an audiovisual speech perception task (Ozker et al., 2018) at high-gamma frequency band. Large trial-to-trial variation necessitates the use of statistical inference to automate the extraction of both the population trajectories and supports of underlying brain activities.

Over the past several decades, there has been an extensive literature on sparsity. This leads to a rich menu of methods in the context of regularization-based variable selection, including adaptive lasso (Zou, 2006), SCAD (Fan and Li, 2001), elastic net (Zou and Hastie, 2005), Dantzig selector (Candes and Tao, 2007), non-concave MCP penalty (Zhang, 2010), and bridge regression (Knight and Fu, 2000). Such concepts have been recently extended to nonparametric estimation of sparse functions; see Barber et al. (2017); Chen et al. (2016); Fan and Reimherr (2017); Huang et al. (2010); Lin et al. (2017). However, little work has been done for functions with local sparsity. A few exceptions include James et al. (2009), which pioneers the method of “FLiRTI” using a grid basis to approximate the nonparametric function. Zhou et al. (2013) proposes a two-stage approach and applied the Dantzig selector followed by group-SCAD. Lin et al. (2017) combines functional SCAD regularization and smoothing splines in a single optimization objective function, achieving smooth and locally sparse estimators simultaneously. Wang and Kai (2015) and Wang and Wang (2017) utilize the group bridge penalty that has been studied by Huang et al. (2008, 2009). However, all of these methods rely on scalar responses and are not suitable for the motivating iEEG studies, where the response is functional and covariate is scalar; we refer to such cases as function-on-scalar regression hereafter. On the other hand, function-on-scalar regression poses unique challenges when developing methodology and studying theoretical properties. For example, the intrafunctional dependence of responses is vital, and the large sample properties may be more intricately determined by the sample size (number of subjects) as well as the sampling frequency of individual trajectories of each subject.

In this paper, we study the problem of simultaneous regression and support estimation under the function-on-scalar setting, where the response is functional, each covariate is scalar, and intrafunctional dependence of responses is vital. We adopt group bridge estimators coupled with B-splines to recover the sparse pattern of function regression coefficients. The proposed method does not require Gaussian assumptions and allows flexible within-curve correlation structures, where we use phase-dependent random effects to account for the heterogeneity in the functional observation. This leads to a novel *weighted functional group bridge* approach for function-on-scalar mixed effect models. In numerical studies, we introduce a nested alternating direction method of multipliers (ADMM) algorithm with early stopping to speed up the computation. The proposed methods possess desirable theoretical properties in terms of convergence rate and sparsistency. We show that under mild conditions, the L_2 and L_∞ (supremum) convergence rate match with minimax-rates asymptotically. Under such conditions, δ -sparsistency and strict sparsistency are established. Although under different models, our theory relies on substantially simplified assumptions than the existing literature to regularize regression functions, notably Assumption 2, which tend to be more interpretable. We consider flexible sampling designs to account for broad applications, including one where the number of time points grows faster than the sample size, which is better suited for iEEG studies. In an application to the aforementioned iEEG experiment, our results complement previous studies by showing that multisensory interac-

tions are a powerful modulator of activity throughout the speech perception network (Karas et al., 2019; Ozker et al., 2018). The proposed methods have been integrated into the newest version of RAVE (Wang et al., 2020), an R package that gains increasing popularity in the iEEG community.

The rest part of this paper is organized as follows. In Section 2 we introduce the model and the estimation procedure, as well as the numeric convergence of the proposed algorithm. Section 3 provides asymptotic properties. In Section 4 we conduct a simulation, followed by real data application to iEEG analysis in Section 5. All the proofs are included in Section 6.

2 Methodology

2.1 Model

Suppose a sample of n functional signals $\{y_i(t)\}_{i=1}^n$ is observed on a compact time set \mathcal{T} . We assume without loss of generality $\mathcal{T} = [0, 1]$. The linear function-on-scalar mixed effect model assumes

$$y_i(t) = \sum_{j=1}^p x_{ij} \beta_j(t) + \theta_i(t) + \epsilon_i(t), \quad (1)$$

where x_{ij} is a scalar predictor, $\beta_j(t)$ is a fixed effect function, $\theta_i(t)$ is random effect with zero means and covariance kernel $\Sigma_\theta^*(t, t')$, and $\epsilon_i(t)$ is the error function independent of $\theta_i(t)$ with zero means and covariance kernel $\Sigma_\epsilon^*(t, t')$. We assume $\beta_j(t)$ is smooth and locally sparse on the time domain. We propose to use phase-dependent random effects to account for heterogeneous dependence structures in various stages of an experiment, such as resting phase, trial onset, and stimuli offset. In particular, we partition \mathcal{T} into a union of disjoint intervals $\{\mathcal{T}^{\text{pa}}\}_{\text{pa}=1}^P$, where each \mathcal{T}^{pa} corresponds to a stage of the experiments, and assume $\theta_i(t)$ is self-correlated but independent across observations. This generalizes the traditional mixed effect models where P is one.

We use B-splines $\{\phi_k(t)\}_{k=1}^K$ to approximate each fixed effect function, that is, $\beta_j(t) = \sum_{k=1}^K \gamma_{jk} \phi_k(t)$ up to approximation error $R_j(t)$. In addition to sharp approximation bounds to smooth functions, B-splines are particularly well suited for sparse functions as they are locally supported and thus transfer sparsity in $\beta(t)$ to a sparse p by K matrix $\gamma = \{\gamma_{jk}\}_{p \times K}$. Let a non-negative integer d be the degree of B-splines and define the knots of length $K+d+1$ be $t_{m_1} = \dots = t_{m_d} = 0 = t_{m_{d+1}} < t_{m_{d+2}} < \dots < t_{m_K} = 1 = t_{m_{K+1}} = \dots = t_{m_{K+d+1}}$, then B-splines are defined recursively as in De Boor (1978):

$$\begin{aligned} \phi_{k,1}(t) &= \begin{cases} 1 & t_{m_k} \leq t < t_{m_{k+1}} \\ 0 & \text{otherwise} \end{cases} \\ \phi_{k,q}(t) &= \frac{t - t_{m_k}}{t_{m_{k+q-1}} - t_{m_k}} \phi_{k,q-1}(t) + \frac{t_{m_{k+1}} - t}{t_{m_{k+q}} - t_{m_{k+1}}} \phi_{k+1,q-1}(t). \end{aligned}$$

B-spline basis functions of order $q = d + 1$ are $\phi_k(t) = \phi_{k,q}(t)$ for $k = 1, \dots, K$. We choose B-spline basis functions with orders at least $q \geq 4$.

In practice, functional data are observed at discrete time points. Let $\mathcal{T}_0 = \{t_m\}_{m=1}^T \subseteq \mathcal{T}$ be the set of time points at which $y_i(t)$ is observed. Each partition set $\mathcal{T}_0^{\text{pa}}$ is defined as

$\mathcal{T}_0 \cap \mathcal{T}^{\text{pa}}$. Let $Y = \{y_{im}\}_{n \times T}$, $\theta = \{\theta_{im}\}_{n \times T}$, $E = \{e_{it}\}_{n \times T}$ be the discretized responses, random effects, and random noise observed at \mathcal{T}_0 , respectively, and $X = \{x_{ij}\}_{n \times T}$ the design matrix, $B = \{B_k^m\}_{K \times T}$ the basis functions $\{\phi_k(t)\}_{k=1}^K$ evaluated on \mathcal{T}_0 , and $R = \{R_j(t_m)\}_{p \times T}$ the corresponding approximation error. Then Model (1) can be written as

$$Y = X\gamma B + XR + \theta + E,$$

where θ and E have covariance Σ_θ and Σ_ϵ that are discretized $\Sigma_\theta^*(t, t')$ and $\Sigma_\epsilon^*(t, t')$ on \mathcal{T}_0 .

In what follows, we use subscript to index rows; for example, Y_i, X_i, γ_j, B_k are the corresponding rows of Y, X, γ, B , respectively. We use $B^{(m)}$ to denote the m^{th} column of B , and $X^{(j)}$ to denote the j^{th} column of X . All vectors are column vectors.

2.2 Estimation: Weighted functional group bridge

We propose to estimate $\beta(t)$ by $\hat{\beta}(t) = \hat{\gamma}\phi(t)$, where $\hat{\gamma}$ as an estimator of γ is obtained by minimizing a penalized weighted squared error,

$$\hat{\gamma} = \underset{\gamma}{\operatorname{argmin}} L(\gamma; \lambda, \alpha, W) = \underset{\gamma}{\operatorname{argmin}} \{f(\gamma; W) + \lambda g(\gamma; \alpha)\}; \quad (2)$$

here $f(\gamma; W) = \frac{1}{2} \sum_{i=1}^n \|(Y_i^T - X_i^T \gamma B)W\|_2^2$ is the squared error loss with each observation weighted by a $T \times T$ matrix W , and $\lambda g(\gamma; \alpha)$ is a penalty term to encourage sparsity on γ with tuning parameters $\lambda \geq 0, \alpha > 0$.

We indicate with the column vector $\mathbf{1}(B^{(m)}) = \{\mathbf{1}(B_k^{(m)})\}$ the indicator function evaluated on $B^{(m)}$, i.e., its k th element $\mathbf{1}(B_k^{(m)}) = 1$ if $B_k^{(m)} \neq 0$, and zero otherwise. We further decompose $g(\gamma; \alpha)$ into pT groups to allow flexible sparsity structures for each $\beta_j(t)$:

$$g(\gamma; \alpha) = \sum_{j=1}^p \sum_{m=1}^T g_{j,m}(\gamma; \alpha), \quad g_{j,m}(\gamma; \alpha) = \|\mathbf{1}(B^{(m)}) \odot \gamma_j\|_1^\alpha = \left[\sum_{k=1}^K |\gamma_{jk}| \cdot \mathbf{1}(B_k^{(m)}) \right]^\alpha, \quad (3)$$

where $\|\cdot\|_1$ is the L_1 norm, and $\mathbf{1}(B^{(m)}) \odot \gamma_j$ is the element-wise multiplication between $\mathbf{1}(B^{(m)})$ and γ_j . The grouped penalty $g(\gamma)$ in Equation (3) shrinks γ and subsequently $\beta(t)$ towards zero. Within each group, the L_1 penalty $\|\mathbf{1}(B^{(m)}) \odot \gamma_j\|_1$ on a subset of γ leads to sparse estimates $\hat{\gamma}$ (Tibshirani, 1996). At the group level, if $g_{j,m}(\gamma; \alpha) = 0$, then $|\beta_j(t_m)| = |\gamma_j^T B^{(m)}| = 0$, hence each group $g_{j,m}(\gamma; \alpha)$ can be interpreted as sparse constraint imposed at time t_m . With $\alpha > 0$, the penalty $g_{j,m}(\gamma; \alpha) = \|\mathbf{1}(B^{(m)}) \odot \gamma_j\|_1^\alpha$ induces a bridge penalty on $\beta_j(t_m)$ (Fu, 1998). Knight and Fu (2000) shows bridge estimators with $\alpha \in (0, 1]$ combine variable selection and parameter estimation in a single step when λ is sufficiently large. Huang et al. (2008) and Park and Yoon (2011) show in their studies $\alpha < 1$ outperforms Lasso in appropriately distinguish between nonzero and zero coefficients in sparse high-dimensional settings. The selection of α and λ is crucial to adapt to the sparsity in γ ; we propose a modified extended Bayesian information criterion to tune these two parameters in Section 2.5.

The weight matrix W accounts for heterogeneity in the functional response. We propose to use $W \propto \Sigma^{-1/2}$, where $\Sigma = \Sigma_\theta + \Sigma_\epsilon$ is the covariance matrix of $Y_i^T - X_i^T \beta$, which reduces the weighted functional group bridge in Equation (2) to an unweighted version after rescaling

in view of that the covariance of $(Y_i^T - X_i^T \beta)W$ is proportional to the identity matrix. The covariance matrices Σ_θ and Σ_ϵ , as well as Σ , are typically unknown. We employ local linear regression (Fan, 1993; Zhu et al., 2014) to estimate Σ under assumptions that second-order derivative for $\theta_i(t)$ exists and Σ_ϵ is diagonal. Denote $\Delta_{m,b}(t) = (t_m - t)/b$, $\theta'_{i,b}(t) = b \cdot d\theta_i/dt(t)$, and kernel function $K_b(t_m - t)$, where b is the bandwidth parameter minimizing generalized cross-validation score (Zhu et al., 2014). For each $t \in \mathcal{T}^{\text{pa}}$, we estimate $\theta_i(t)$ using a weighted least squares procedure (Fan, 1993):

$$\begin{aligned} \left(\hat{\theta}_i(t), \hat{\theta}'_i(t) \right)^T = & \underset{\theta_i(t), \theta'_i(t)}{\operatorname{argmin}} \sum_{m: t_m \in \mathcal{T}^{\text{pa}}} \left\{ y_i(t_m) - \sum_{j=1}^p X_{ij} \hat{\beta}_j^{\text{ols}}(t_m) \right. \\ & \left. - [\theta_i(t) + \theta'_i(t) \Delta_{m,b}(t)] \right\}^2 K_b(t_m - t), \end{aligned}$$

where $\hat{\beta}_j^{\text{ols}}(t_m)$ is ordinary least square estimator of the j^{th} coefficient at time t_m . We then calculate the sample covariance of $\{\hat{\theta}_i(t_m)\}_{i,m}$ to estimate Σ_θ on each partition set \mathcal{T}_0 , and the residuals $y_i(t_m) - \sum_{j=1}^p X_{ij} \hat{\beta}_j^{\text{ols}}(t_m) - \hat{\theta}_i(t_m)$ to estimate Σ_ϵ on \mathcal{T}_0 .

To ease notation, in the sequel we omit (α, λ, W) in $L(\gamma; \lambda, \alpha, W)$, $f(\gamma; W)$ and $g(\gamma; \alpha)$ and instead use $L(\gamma)$, $f(\gamma)$, and $g(\gamma)$, respectively, when it does not cause confusion.

2.3 Optimization: Nested ADMM algorithm

Direct minimization of $L(\gamma)$ is well-studied by Huang et al. (2009). They proposed embedding $g(\gamma)$ in a carefully chosen higher dimensional space to transfer this optimization problem to a better studied Lasso problem then link the solution back to $g(\gamma)$ through a particular path. In particular, denote the expanded surface as

$$\begin{aligned} S(\gamma, \zeta) &= \sum_{j,m} s_{j,m}(\gamma, \zeta), \quad \zeta = \{\zeta_{j,m}\}, \\ s_{j,m}(\gamma, \zeta) &= \frac{\alpha^\alpha}{(1-\alpha)^{\alpha-1}} \zeta_{j,m}^{1-\frac{1}{\alpha}} \|\mathbf{1}(B^{(m)}) \odot \gamma_j\|_1 + \alpha^\alpha (1-\alpha)^{1-\alpha} \zeta_{j,m}, \end{aligned}$$

by connecting ζ and γ with $\zeta(\gamma) = \{\zeta_{j,m}(\gamma)\}$, where

$$\zeta_{j,m}(\gamma) = \left(\frac{1-\alpha}{\alpha} \right)^\alpha \|\mathbf{1}(B^{(m)}) \odot \gamma_j\|_1^\alpha,$$

the original non-convex problem in Equation (2) can be solved by finding the solutions for

$$\underset{\gamma, \zeta}{\operatorname{argmin}} L_S(\gamma, \zeta) \quad \text{subject to} \quad \zeta = \zeta(\gamma) \text{ and } \zeta > 0,$$

where $L_S(\gamma, \zeta) = f(\gamma) + S(\gamma, \zeta)$. We carry out the optimization by iteratively updating ζ with fixed $\gamma = \gamma^{\text{old}}$ through the definition $\zeta = \zeta(\gamma)$, updating γ with fixed $\zeta = \zeta^{\text{new}}$, which turns out to be a Lasso problem.

In this paper, we propose to solve the iterative Lasso problem using alternating direction method of multipliers, or ADMM (Boyd et al., 2011). Compared to LARS (Efron et al., 2004) adopted by Huang et al. (2009). The performance can be significantly improved by ADMM

with the use of “warm-start”: If initialized near the solution, usually the solution from the previous loops, ADMM converges faster to modest accuracy within very few steps (Boyd et al., 2011). To fully take the advantage of this property, we early terminate ADMM instead of waiting till fully convergence. Algorithm 1 details the optimization steps. We introduce a few notations before describing Algorithm 1. For any matrix A , let A^+ be the positive part and A^- be its negative part. If A is a square matrix, $\text{diag}(A)$ extracts its diagonal elements into a vector, and $\text{diag}([a_{11}, a_{22}, \dots, a_{pp}])$ expands a vector to a diagonal square. The operator \odot between two matrices defines element-wise division.

Algorithm 1 Nested ADMM solver for the case $\alpha \in (0, 1)$

```

1: procedure WEIGHTED FUNCTION GROUP BRIDGE( $X, Y, b, \lambda, \alpha, W$ ) ▷ Inputs
2:   Initialize  $\gamma \leftarrow \gamma^{(0)} \leftarrow \hat{\beta}_{GLS}$ ,  $E \leftarrow Y - X\gamma B$ ;
3:   SVD decompose:  $X = U_X D_X V_X^T$ ,  $BW = U_B D_B V_B^T$ ;
4:   Assign  $V = V_X^T$ ,  $U = U_B$ ,  $Z = \text{diag}(D_X^2) \text{diag}(D_B^2)^T + \rho \mathbf{1}_p \mathbf{1}_K^T$ ;
5:   for  $v$  in  $1, 2, \dots, S_1$  do ▷ Macro-loop: iterative Lasso
6:     Calculate  $D^{(v)} = \{D_{jk}^{(v)}\}$ , where  $D_{jk}^{(v)} = \alpha^\alpha (1 - \alpha)^{1-\alpha} \zeta_{jm}^{1-\frac{1}{\alpha}} (\gamma^{(v-1)}) \cdot \mathbf{1}(B_k^{(m)})$ ;
7:     Initialize  $\eta^{(0)} = \gamma^{(v-1)}$ ,  $\xi^{(0)} = \gamma^{(v-1)}$ ,  $\psi^{(0)} = \xi^{(0)} - \eta^{(0)} = 0$ ;
8:     for  $s$  in  $1, 2, \dots, S_2$  do ▷ ADMM loop, fixed steps
9:        $\xi^{(s)} \leftarrow V^T ([VX^T YW(BW)^T U - \psi^{(s-1)} + \rho V \eta^{(s-1)} U] \odot Z) U^T$ ;
10:       $\eta^{(s)} \leftarrow [\xi^{(s)} + \frac{1}{\rho} V^T \psi^{(s-1)} U^T - \frac{\lambda}{\rho} D^{(v)}]^+ - [\xi^{(s)} + \frac{1}{\rho} V^T \psi^{(s-1)} U^T + \frac{\lambda}{\rho} D^{(v)}]^-$ ;
11:       $\psi^{(s)} \leftarrow \psi^{(s-1)} + \rho V (\xi^{(s)} - \eta^{(s)}) U$ ;
12:    end for
13:    Assign  $\gamma \leftarrow \gamma^{(v)} \leftarrow \eta^{(S_2)}$ ;
14:    Recall  $\hat{Y} = X\gamma^{(v)} B$ , calculate  $\hat{E} = Y - \hat{Y}$ ;
15:    if  $\|\hat{E}W\|_2$  is stable then ▷ Exit criteria
16:      Break the loop;
17:    end if
18:  end for
19:  Return  $\gamma$ ;
20: end procedure

```

It is worth noting that by setting $S_2 = 1$ and forcing $D_{jk}^{(v)} = 1$ at each iteration, Algorithm 1 also solves the case where $\alpha = 1$.

2.4 Variance Estimation

Algorithm 1 solves an augmented Lagrangian problem L^{aug} :

$$L^{\text{aug}}(\xi, \zeta, \psi, \eta; W, \lambda, \alpha, \rho) = L_S(\xi, \zeta) + \left[\text{vec}(\psi)^T \text{vec}(V\xi U - V\eta U) \right] + \frac{\rho}{2} \|V(\xi - \eta)U\|_2^2,$$

where $\text{vec}(A)$ vectorizes A by stacking columns of A for any matrix A . The dual feasibility in the ADMM optimality condition yields

$$(V\xi^{(s)}U) \odot Z = VX^T YW W^T B^T U - \psi^{(s-1)} + \rho V \eta^{(s-1)} U \quad (4)$$

$$\mathbf{0} = \left[-\frac{\lambda}{\rho} D(\zeta) \text{sign}(\xi^{(s)}) + \frac{1}{\rho} V^T \psi^{(s-1)} U^T - \eta^{(s)} \right] \odot \text{sign}(\xi^{(s)}). \quad (5)$$

When Algorithm 1 converges, $\rho(\eta^{(s)} - \eta^{(s-1)}) \rightarrow \mathbf{0}$ and $\xi^{(s)} \rightarrow \hat{\gamma}$, there for (j, k) s.t. $\hat{\gamma}_{jk} \neq 0$, optimality conditions (4) and (5) yields

$$X^{(j)T} X \hat{\gamma} B W W^T B_k + \lambda D_{jk}(\hat{\zeta}) \hat{\gamma}_{jk} = X^{(j)T} X \gamma B W W^T B_k + X^{(j)T} E W W^T B_k. \quad (6)$$

Denote $P(j, k) = \text{vec}(X^T X^{(j)} B_k^T W W^T B^T + \lambda D_{jk} J(j, k))$, where $J(j, k)$ is sparse matrix with only its (j, k) element being 1, and let $Q(j, k) = X^{(j)} B_k^T W W^T$. Then (6) can be written as

$$\text{vec}[P(j, k)]^T \text{vec}(\hat{\gamma}) = \text{vec}[Q(j, k)]^T \text{vec}(X \gamma B + Z \theta + E),$$

for (j, k) s.t. $\hat{\gamma}_{jk} \neq 0$. Letting $\text{vec}_\lambda(\hat{\gamma})$ be the sub-vector of $\text{vec}(\hat{\gamma})$ on its support, that is, all elements in $\text{vec}_\lambda(\hat{\gamma})$ are non-zeros, and $P_\lambda(j, k)$ be $P(j, k)$ on its support, then we have $\text{vec}[P(j, k)]^T \text{vec}(\hat{\gamma}) = \text{vec}_\lambda[P(j, k)]^T \text{vec}_\lambda(\hat{\gamma})$. Bind $\text{vec}_\lambda[P(j, k)]$ by column for all (j, k) s.t. $\hat{\gamma}_{jk} \neq 0$, and denote it as P_λ . It is easy to show that P_λ is a square matrix and further $P_\lambda \text{vec}_\lambda(\hat{\gamma}) = Q \text{vec}(X \gamma B + Z \theta + E)$, where Q is also a square matrix column-binded by $\text{vec}[Q(j, k)]$. Consequently, the covariance of $\hat{\gamma}$ is given by

$$\text{Cov}[\text{vec}_\lambda(\hat{\gamma})] = P_\lambda^{-1} Q \text{Cov}[\text{vec}(Z \theta + E)] Q^T (P_\lambda^T)^{-1}. \quad (7)$$

2.5 Parameter tuning: Adjusted EBIC

We choose an equally spaced sequence of knots for B-splines. For given K , we adopt the extended BIC (EBIC) framework proposed by Chen and Chen (2008) but introduce adjustments to improve upon finite sample performance in addition to incorporating the weight matrix W :

$$EBIC_\nu = \frac{\|(Y - X \hat{\beta})W\|_2^2}{n\sigma^2} + T \log(\sigma^2) + df \frac{\log n}{n} + \nu df \frac{\log pK}{n},$$

where $\hat{\beta}$ is the fitted coefficients of given model, df is number of non-zero elements in γ , ν is a constant between $[0, 1]$, in which we suggest $\nu = \max\{1 - \frac{\log(n)}{2 \log(pK)}, \frac{1}{2}\}$ based on Theorem 1 and discussions in Chen and Chen (2008), and σ^2 is an unknown parameter analogue to the error variance in a standard regression model. Huang et al. (2010) and Wang and Kai (2015) substituted $n\sigma^2$ with residual sum of squares based on $\hat{\beta}$. Since a bridge estimator is not unbiased due to its shrinkage to zero, we instead propose to estimate σ^2 by the weighted residual sum of squares based on the generalized least-square estimator $\hat{\beta}_{GLS}$, which does not possess sparsity but is unbiased. In particular, we have $\hat{\beta}_{GLS} = (X^T X)^{-1} X^T Y W W^T B^T (B W W^T B^T)^{-1}$, and

$$\hat{\sigma}_{GLS}^2 = \frac{1}{nT} \|(Y - X \hat{\beta}_{GLS})W\|_2^2.$$

This leads to an adjusted EBIC

$$EBIC_\nu = T \frac{\|(Y - X \hat{\beta})W\|_2^2}{\|(Y - X \hat{\beta}_{GLS})W\|_2^2} + df \frac{\log n}{n} + \nu df \frac{\log pK}{n}, \quad (8)$$

up to an additive constant. In the simulation, we observe that our proposed adjusted EBIC selects parameters that give more accurate estimation than EBIC (weighted or unweighted

by W). In addition, the adjusted EBIC tends to select parameters that are close to the oracle values; see Section 4 for more details.

We recommend to the proposed adjusted EBIC to both α and λ . Although this might be time consuming, we observe that it usually gives robust selections. One can also fix α and only tune λ using the adjusted EBIC, especially when computational time is a concern. Indeed, most works on bridge penalties consider to use an arbitrary but fixed $\alpha \in (0, 1)$ that is bounded away from 0 and 1, for example, by letting $\alpha = 0.5$ (Huang et al., 2008). In general, there is a lack of theory concerning the proper choice of α ; in the next section we include discussions to guide choosing α based on large sample theory when such specification is preferred in practice.

3 Asymptotic Properties

In this section, we study asymptotic properties of the proposed estimators. Let $\{\beta_j^*(t)\}_{j=1}^p$ be the underlying true function coefficients in Model (1). For a function $f(t) : [0, 1] \rightarrow \mathbb{R}$, let $\|f\|_r$ be the L_r norm and $\|f\|_\infty = \sup_{t \in [0, 1]} |f(t)|$. Let $\mathcal{C}^r[0, 1]$ be the Hölder space on $[0, 1]$ with order r that consists of all functions $f(t)$ such that for some $L_f > 0$, $|f^{(r_0)}(x) - f^{(r_0)}(y)| \leq L_f \|x - y\|^{r-r_0}$ for all $x, y \in [0, 1]$, where r_0 is the largest integer strictly smaller than r . Let $\delta_{\min}(A)$ and $\delta_{\max}(A)$ be the minimum and maximum eigenvalues for any given matrix A . For two sequences $a_{n,T}$ and $b_{n,T}$, $a_{n,T} \lesssim b_{n,T}$ means $a_{n,T} \leq Cb_{n,T}$ for some universal constant $C > 0$. We write $a_{n,T} \asymp b_{n,T}$ if $a_{n,T} \lesssim b_{n,T}$ and $a_{n,T} \gtrsim b_{n,T}$. Asymptotics in this section are interpreted when n and T go to infinity.

We assume the following regularity conditions.

Assumption 1. *The underlying $\beta_j^*(t) \in \mathcal{C}^r[0, 1]$, for $j = 1, 2, \dots, p$ and $r \geq 2$.*

Assumption 2. *The integral $\int_{\beta_j \neq 0} |\beta_j^*(t)|^{2\alpha-2} dt$ exists and is finite, for all j .*

Assumption 3. *$\{\epsilon_i(t)\}_{i=1}^n$ and $\{\theta_i(t)\}_{i=1}^n$ are independent across i and sub-Gaussian.*

Assumption 4. *The design matrix satisfies that for some constants $C_1, C_2 > 0$, $C_1 \leq \delta_{\min}(X^T X/n)$ and $\delta_{\max}(X^T X/n) \leq C_2$, and the weight matrix is chosen such that $C_3 \leq \delta_{\min}(WW^T) \leq \delta_{\max}(WW^T) \leq C_4$ for some constants $C_3, C_4 > 0$, for all sufficiently large n and T .*

Assumption 5. $\max_m (t_{m+1} - t_m) = O(T^{-1})$.

Assumption 6. $C_5 K^{-1} \leq t_{m_{k+q}} - t_{m_k} \leq C_6 K^{-1}$ for some constants $C_5, C_6 > 0$, where $K < T$.

Assumptions 1, 3, 4, and 5 are common in functional data analysis. The assumption on W trivially holds if W is chosen as the identity matrix that corresponds to the unweighted implementation of the proposed method. Without loss of generality, we assume that $\delta_{\max}(WW^T) = 1$. Assumption 6 spells out a mild condition on B-splines to avoid singularity issues, and it trivially holds if all knots are equally spaced. A close inspection of the proofs of the subsequent theorems indicates that they all hold if Assumption 4 is concerned with random X and W but satisfied with probability approaching one.

Assumption 2 is in the same vein of Conditions (B') and (C') in Fan and Peng (2004) to ensure that the group bridge penalty does not dominate the least square error on its support, and implies that $\beta_j^*(t)$ deviates from zero fast enough so that its support and zero set can be well distinguished. Unlike Fan and Peng (2004); Huang et al. (2009), Assumption 2 disentangles the penalty and the regression function, leading to a simpler and more interpretable formulation to regularize regression coefficients. We achieve such simplicity by relying on a carefully modified B-spline approximation that will be detailed in Lemma 6.2. This assumption also suggests a lower bound of α for $\beta_j^*(t)$ leaving zeros at polynomial speed. If $\beta_j^*(t_0) = 0$ for some t_0 and $\beta_j^*(t)$ satisfies $|\beta_j^*(t)| \gtrsim |t - t_0|^b$ as t approaches t_0 for some positive constant b , then choosing $\alpha > 1 - 1/(2b)$ is required to comply with this assumption.

It is well known that if $\beta_j^*(t) \in C^r[0, 1]$ and there are no overlapping spline knots for t_{m_k} for $q \leq k \leq K$, then there exists a B-spline approximation such that L_∞ approximation error is upper bounded by K^{-r} up to a constant; for example, see Schumaker (2007). However, these accurate B-spline approximations do not necessarily capture the sparsity of the true function. In Lemma 6.2, we propose a sparse modification of such B-splines so that the new approximation, denoted as $\tilde{\beta}_j(t) := \sum_{k=1}^K \tilde{\gamma}_{jk} \phi_k(t)$, preserves sparsity with $\|\tilde{\beta}_j(t) - \beta_j^*(t)\|_\infty \leq C_{\beta_j} K^{-r}$ for some constant C_{β_j} . We call the modified B-spline coefficients $\hat{\gamma} = \{\tilde{\gamma}_{jk}\}_{p \times K}$ pseudo true values of γ . The triangle inequality gives

$$\begin{aligned} \|\beta_j^*(t) - \hat{\beta}_j(t)\|_\infty &\leq \|\beta_j^*(t) - \tilde{\beta}_j(t)\|_\infty + \|\tilde{\beta}_j(t) - \hat{\beta}_j(t)\|_\infty \\ &\leq C_{\beta_j} K^{-r} + \|\hat{\gamma} - \tilde{\gamma}\|_\infty \sum_{k=1}^K \|\phi_k(t)\|_1, \end{aligned}$$

where $\sum_{k=1}^K \|\phi_k(t)\|_1 = 1$. Therefore, convergence rates of $\hat{\beta}(t)$ boils down to convergence rates of $\hat{\gamma}$ relative to the pseudo true $\tilde{\gamma}$, as well as the approximation error $C_{\beta_j} K^{-r}$ of using B-splines. The following Theorem 3.1 and Theorem 3.2 establish convergence rates of $\hat{\gamma}$ and $\hat{\beta}_j$. In the following theorems, without loss of generality we relate K, T to n by writing $K = n^{\frac{\kappa}{2r}}$ and $T = n^{\frac{\tau}{2r}}$ where $0 < \kappa \leq \tau$. It is worth mentioning that $n^{\frac{\kappa}{2r}}$ and $n^{\frac{\tau}{2r}}$ represent the asymptotic rates of K and T , and any multiplicative constants do not change our results, i.e., we here set the multiplicative constants to be one to ease notation. To state the two theorems in their most general forms, we do not yet assume a specific order of either κ or τ .

Theorem 3.1 (Convergence rate of $\hat{\gamma}$). *Letting $c_\kappa = \min(1, \kappa)$, under Assumptions 1- 6, if $\frac{\log(\lambda)}{\log(n)} \leq 1 - \frac{c_\kappa}{2} + \frac{\tau}{4r} - \frac{\kappa}{4r}$, then we have as $n \rightarrow \infty$*

$$\|\hat{\gamma} - \tilde{\gamma}\|_\infty \leq \|\hat{\gamma} - \tilde{\gamma}\|_2 = O_p(n^{\frac{\kappa}{4r} - \frac{c_\kappa}{2}}).$$

Combining Theorem 3.1 and Lemma 6.1, in Theorem 3.2 we obtain convergence rates of $\hat{\beta}(t)$ under both L_2 and L_∞ norms for functional coefficients.

Theorem 3.2 (Convergence rates of $\hat{\beta}(t)$). *Under the same assumptions of Theorem 3.1, as $n \rightarrow \infty$,*

$$\|\hat{\beta}_j(t) - \beta_j^*(t)\|_\infty = O_p(n^{\frac{\kappa}{4r} - \frac{c_\kappa}{2}}), \quad (9)$$

$$\|\hat{\beta}_j(t) - \beta_j^*(t)\|_2 = O_p(n^{-\frac{c_\kappa}{2}}). \quad (10)$$

We remark that there is a phase transition at $\tau = 1$ in Equation (9). When $\tau < 1$, because $\kappa < \tau$, we have $c_\kappa = \kappa$, and the optimal L_∞ rate is attained at the largest κ , i.e., $\kappa = \tau$, which gives the rate $O_P(n^{(1-2r)\frac{\tau}{4r}})$. In this case, the rate improves as τ increases. When $\tau > 1$, the optimal L_∞ rate is $O_P(n^{(1-2r)\frac{1}{4r}})$, which is achieved at $\kappa = 1$, and increasing τ does not improve the rate. The same phase transition also applies to the L_2 rate in Equation (10), which coincides with the observations made in Cai and Yuan (2011). In addition, the rate calculation implies one may choose $\kappa = \min(\tau, 1)$. Such choice of κ leads to a rate of $O_P(n^{-\min(\tau, 1)/2})$, i.e., $O_P(n^{-1/2} + T^{-r})$ under the L_2 norm using Equation (10), which is minimax optimal (Cai and Yuan, 2011).

The rate under the L_∞ norm in equation (9) indicates that $\hat{\beta}(t)$ converges to $\beta^*(t)$ at each t as n for $\kappa < 2r$. This is particularly useful in detecting sparse regions as pointwise convergence suggests low false positive rates and low false negative rates in finding the underlying support of $\beta_j^*(t)$. In particular, let $S(h) = \{t \in \mathcal{T} : h(t) = 0\}$ map a function $h(\cdot)$ to its zero set and we additionally consider δ -sparsity induced by $S_\delta(h) = \{t \in \mathcal{T} : |h(t)| \leq \delta\}$ for $\delta > 0$. Then the rate in Equation (9) suggests that for arbitrary $\delta > 0$, as $n \rightarrow \infty$,

$$P\{S(\hat{\beta}_j) \subset S_\delta(\beta_j^*)\} \rightarrow 1, \quad P\{S(\hat{\beta}_j^*) \subset S_\delta(\beta_j)\} \rightarrow 1.$$

In addition, our proposed method achieves low false positive rates under strict sparsity, that is, the support of $\hat{\beta}(t)$ is a subset of $\beta_j^*(t)$ with probability approaching to 1, or equivalently $S(\beta_j^*) \subseteq S(\hat{\beta}_j)$ using the complement of supports. Theorem 3.3 formulates such a result.

Theorem 3.3. *Under the same conditions assumed in Theorem 3.1 and $\frac{\log(\lambda)}{\log(n)} > 1 + \frac{c_\kappa(\alpha-2)}{2} + \frac{\tau}{2r} - \frac{\kappa\alpha}{4r}$, as $n \rightarrow \infty$, there holds for any $\delta > 0$,*

$$P\{S(\beta_j^*) \subset S(\hat{\beta}_j)\} \rightarrow 1.$$

Under Assumptions 1-6, there is a hidden condition for Theorem 3.3 to hold: $\alpha < 1 - \frac{\tau}{2rc_\kappa - \kappa}$. For α too close to 1, this condition fails and we might be unable to fully recover the sparsity. In addition, Assumption 2 is more likely to be satisfied when α is large. Therefore we propose α to be slightly less than $1 - \frac{\tau}{2rc_\kappa - \kappa}$ in the real data application. By letting $\kappa = \min(\tau, 1)$, when the estimators are minimax optimal under the L_2 norm, we propose $\lambda \asymp n^{1 + \frac{\tau}{4} - (\frac{1}{2} + \frac{1}{4r})\min(1, \tau)}$ and $\alpha < 1 - \frac{\max(\tau, 1)}{2r-1}$.

4 Simulations

We conduct simulations to compare finite sample performances of the proposed approach with competing methods in terms of function estimation and sparse region detection. We also assess the the proposed adjusted EBIC method for parameter tuning.

We generate data according to Model (1). We consider three coefficients to represent different sparsity levels, displayed in Figure 2: $\beta_1(t) = 0$ for global sparsity, $\beta_2(t) = \sin(\pi t)$ for no sparsity (a dense coefficient), and $\beta_3(t)$ for local sparsity that is defined as

$$\beta_3(t) = \begin{cases} 0 & t \in [0, 0.2) \cup [0.8, 1] \\ \sin\left(\frac{5\pi}{2}t - \frac{\pi}{2}\right) & t \in [0.2, 0.4) \\ 1 & t \in [0.4, 0.6) \\ \sin\left(\frac{5\pi}{2}t - \pi\right) & t \in [0.6, 0.8). \end{cases}$$

Note that among the three coefficient functions $\beta_3(t)$ is the most interesting one as it is locally sparse that pertains to the motivation of this paper; $\beta_1(t)$ and $\beta_2(t)$ are not of particular interest, but we include them in the data generating procedure to study the performances of the proposed method in various scenarios, and especially to assess each method on $\beta_3(t)$ when there are other coefficient functions at various sparsity levels. The design matrix X is generated from the standard normal distribution $N(0, 1)$. To simulate different phases of experiments, the random effects $\theta_i(t)$ are generated from a $AR(1) \times \sigma(t)$ process, where $\sigma(t)$ is a non-decreasing step function visualized in Figure 2 and $AR(1)$ is an order one autoregressive process with correlation 0.9. The errors $\epsilon_i(t_m) \sim N(0, 1)$ are independently across observations and time points. We use $T = 100$ as the time resolution to generate equally spaced t_m . We consider two sample sizes: $n = 100$ (small sample size) and $n = 1000$ (large sample size). We run 100 simulations for each sample size.

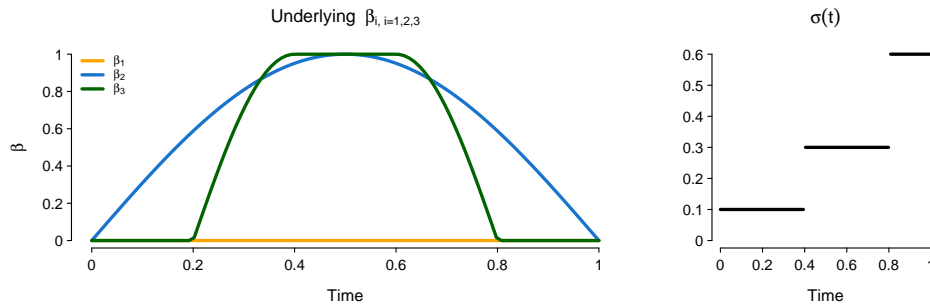


Figure 2: Three coefficient functions (left) and step function $\sigma(t)$ (right).

In addition to the proposed weighted function group bridge approach, we include its two variants: homogeneous weight ($W = I$), and $\alpha = 1$. Other competing methods include Group Lasso (gLasso) proposed by Barber et al. (2017), Group MCP (gMCP) by Chen et al. (2016), and two-step function-on-scalar (2-Step FoS) regression (Fan and Zhang, 2000). For the proposed methods, we set $K = 30$ and choose λ and α , when applicable, by minimizing the adjusted EBIC in Equation (8) through a grid search using 100 λ 's chosen log-linearly from 0.1 to 100 and 18 α 's linearly from 0.05 to 0.95. We derive joint confident bands for $\beta(t)$'s based on the variance estimation in Section 2.4. In particular, we perturb sparse estimates $\hat{\gamma}_{jk}$ with small random numbers to expand Equation (7) into all $\hat{\gamma}_{jk}$'s, which gives the covariance of $\hat{\gamma}$ and subsequently a joint confident band for each $\beta(t)$.

Figure 3 provides visual comparisons of all the estimates and their 95% joint confidence intervals. Our proposed method has tighter and more adaptive confidence intervals than gMCP and gLasso as we assume heterogeneous errors. Two-step FoS also enjoys tight joint CIs, but it cannot recover sparsity. Though all other methods contain sparsity constraints in their design, gLasso fails to detect the support of $\beta_1(t)$ and $\beta_3(t)$, while functional group bridge based methods and gMCP succeed in recovering global sparsity $\beta_1(t)$. The proposed method is the only method to recover the locally sparse coefficient $\beta_3(t)$ at $t \in (0.8, 1]$, when the error variance is large, indicating its adaptivity to various sparse levels and variance noise levels.

We next focus on $\beta_3(t)$ and compare each method in terms of both accuracy and sparsity detection. For each method, we calculate the root mean squared error (RMSE) $\|\hat{\beta}_3(t) -$

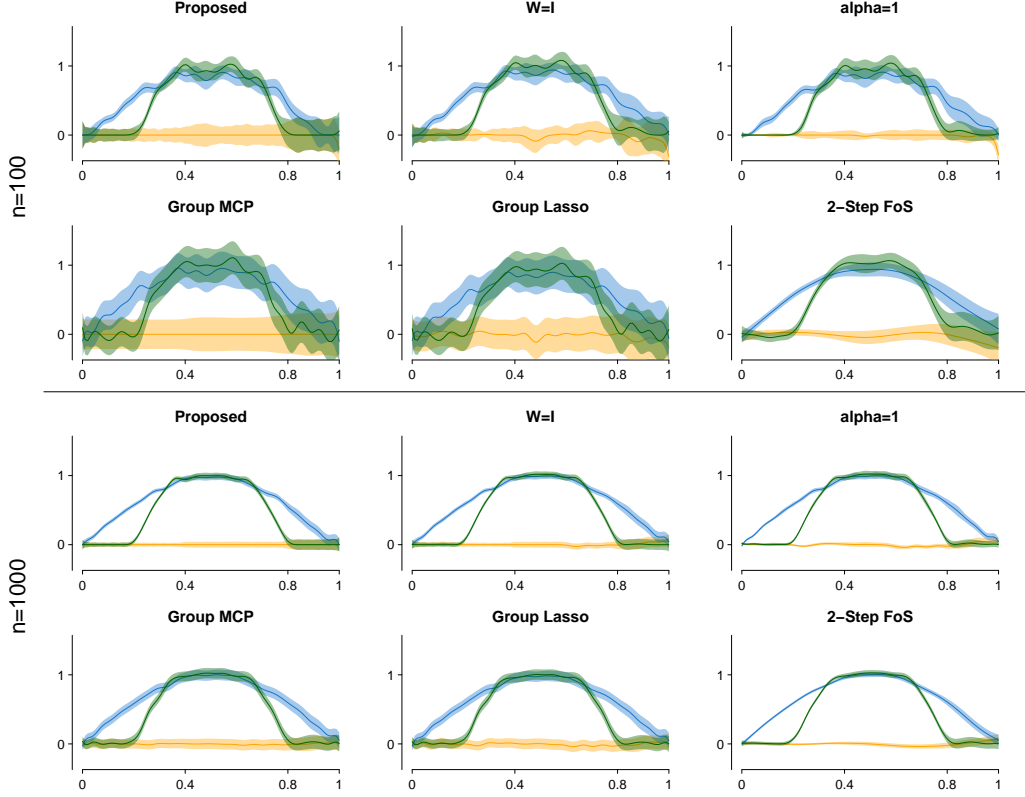


Figure 3: Fitted coefficients with 95% joint confidence intervals at $n = 100$ (top two rows) and $n = 1000$ (bottom two rows).

$\beta_3^*(t)\|_2$ to measure the overall accuracy and $\|\hat{\beta}_3(t) - \beta_3^*(t)\|_\infty$ to measure the maximum difference, reported in Table 1. We can see that our approach outperforms other methods in estimating the locally sparse coefficient $\beta_3(t)$ for both sample sizes. We also calculate the coverage of the confident bands produced by each method. All methods except $\alpha = 1$ attain the nominal coverage after taking the standard errors into account at $n = 1000$. Both gMCP and gLasso lead to the largest coverage at the expense of wider confidence bands; this can be clearly observed in Figure 3. In contrast, the proposed method gives much tighter confidence bands while maintaining a coverage that is close to the nominal level.

Table 2 compares false positive rates (FPRs) for each method. The proposed method leads to the lowest FPR on nearly all time segments that correspond to various noise levels and the entire time domain $[0, 1]$ for both sample sizes; the only exception occurs on $[0, 0.2]$ (small volatility) when $n = 100$, but the difference compared to the best other method $\alpha = 1$ is within 2 standard errors. It is not surprising that 2-Step FoS does not recover sparse regions as it is not designed for sparse functions. Although gMCP and gLasso encourage sparse estimate, the estimated curves have no regions that are exactly zero. The substantial performance gain of the proposed method over $\alpha = 1$ and other competing methods may be partly due to the use of functional group bridge estimators for local sparsity and heterogeneous weight matrix to accounts for volatility changes. Figure 4 shows the mean ROC curve over 100 simulations for $\beta_3(t)$ by varying a threshold to define sparsity. The proposed

method dominates other methods for both sample sizes, suggesting its superior performance under δ -sparsity.

n		Proposed	$W = I$	$\alpha = 1$	gMCP	gLasso	2-Step FoS
100	RMSE $(\times 0.01)$	6.0 (0.2)	6.6 (0.2)	7.0 (0.2)	7.4 (0.2)	8.3 (0.2)	6.4 (0.2)
	$L_\infty (\times 0.1)$	1.8 (0.1)	1.9 (0.1)	1.8 (0.0)	2.1 (0.1)	2.1 (0.1)	1.8 (0.1)
	Coverage (%)	92.3 (0.8)	93.7 (0.5)	82.7 (0.9)	99.6 (0.1)	99.7 (0.1)	93.4 (0.6)
1000	RMSE $(\times 0.01)$	1.8 (0.0)	2.1 (0.1)	2.1 (0.0)	2.4 (0.0)	2.7 (0.1)	2.2 (0.1)
	$L_\infty (\times 0.01)$	5.6 (0.2)	6.2 (0.2)	6.3 (0.2)	7.1 (0.2)	7.2 (0.2)	6.7 (0.2)
	Coverage (%)	95.3 (0.6)	96.1 (0.4)	88.6 (0.6)	99.8 (0.1)	99.6 (0.1)	93.6 (0.5)

Table 1: **RMSE:** $\|\beta_3^*(t) - \hat{\beta}_3(t)\|_2$, measures the overall inaccuracy. **L_∞ norm:** $\|\beta_3^*(t) - \hat{\beta}_3(t)\|_\infty$, measures the maximum error. **Coverage:** pointwise coverage of 95% joint confidence intervals for $\beta_3^*(t)$.

n	Time	Proposed	W=I	alpha=1	gMCP	gLasso	2-Step FoS
100	0 - 0.2	43.4 (2.6)	68.4 (2.5)	39.0 (2.2)	100 (0.0)	100 (0.0)	100 (0.0)
	0.8 - 1	55.4 (3.3)	93.9 (1.6)	84.9 (2.6)	100 (0.0)	100 (0.0)	100 (0.0)
	Overall	49.2 (2.2)	80.8 (1.6)	61.4 (1.8)	100 (0.0)	100 (0.0)	100 (0.0)
1000	0 - 0.2	46.1 (2.7)	71.1 (2.5)	96.7 (1.0)	100 (0.0)	100 (0.0)	100 (0.0)
	0.8 - 1	63.6 (3.1)	95.1 (1.3)	100.0 (0.0)	100 (0.0)	100 (0.0)	100 (0.0)
	Overall	54.6 (2.2)	82.8 (1.5)	98.3 (0.5)	100 (0.0)	100 (0.0)	100 (0.0)

Table 2: False positive rates of $\hat{\beta}_3(t)$. $\hat{\beta}_3(t)$ is considered false positive if $\hat{\beta}_3(t) \neq 0$ but $\beta_3^*(t) = 0$ (i.e., sparse).

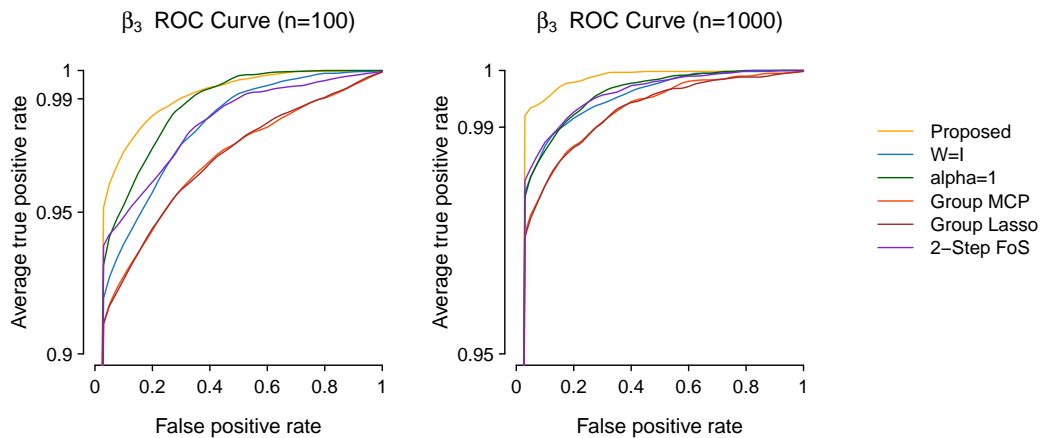


Figure 4: Mean ROC curve for each method at $n = 100$ (left) and $n = 1000$ (right). Results are based on 100 simulations.

Adjusted EBIC. We assess the adjusted EBIC proposed in Section 2.5. Figure 5

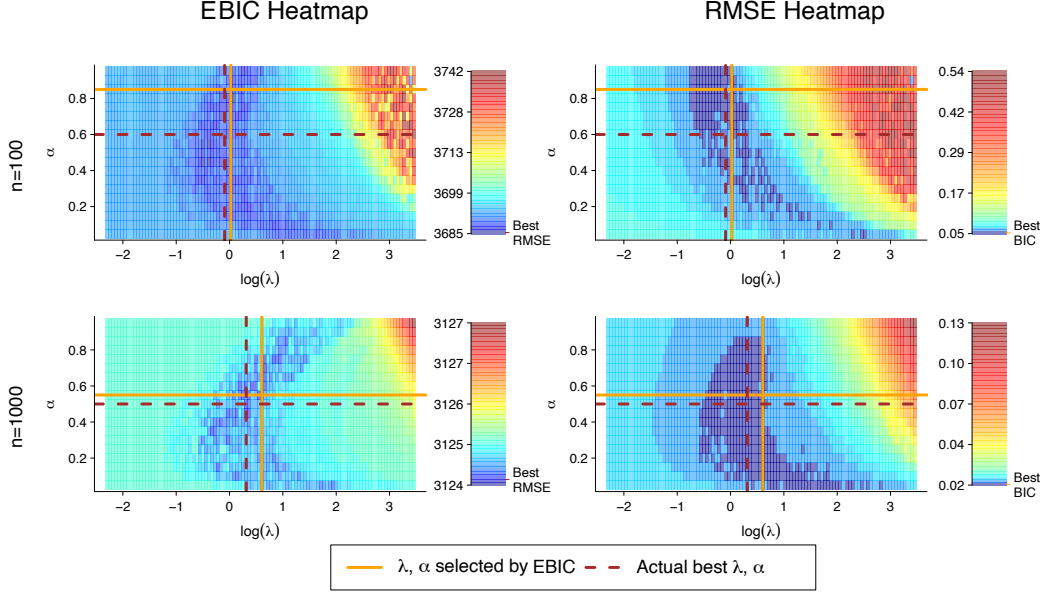


Figure 5: **Left:** Adjusted EBIC heatmap with respect to combinations of (λ, α) . Blue colors suggest small adjusted EBIC. **Right:** Aggregated RMSE $\sum_{j=1}^3 \|\hat{\beta}_j(t) - \beta_j^*(t)\|_2$. Solid orange lines correspond to $(\lambda_{EBIC}, \alpha_{EBIC})$, and dash lines are the optimal (λ, α) .

visualizes the heatmap of adjusted EBIC over (λ, α) along with the aggregated RMSE $\sum_{j=1}^3 \|\hat{\beta}_j(t) - \beta_j^*(t)\|_2$ based on the true functions $\beta_j^*(t)$. The selected parameters according to the adjusted EBIC are marked out by solid cross-lines, and the best combination minimizing the oracle RMSE is marked with dash lines. At $n = 1000$ the adjusted EBIC heatmap is highly consistent with the actual RMSE. The dark blue parts that indicate lowest EBIC and RMSE largely overlap, and the tuned parameters are close to the actual best. For small sample size, although differing from the optimal ones, $(\lambda_{EBIC}, \alpha_{EBIC})$ give low RMSEs. Indeed, the optimal (λ, α) might not be unique as the RMSE heatmaps show a trajectory (dark blue areas in the plot) that achieves the best or close to the best accuracy. This suggests that one may further speed up the tuning step by fixing α and only choosing λ .

5 Application to iEEG Data

In this section, we apply the proposed weighted functional group bridge regression to a human intracranial electroencephalography (iEEG) dataset, which is collected in Beauchamp’s Lab to investigate multisensory integration. In this particular application, we are interested in how different brain areas respond to auditory only versus audiovisual speech.

In this experiment, subjects are asked to watch/listen to a person pronouncing one of the following words: “last”, “drive”, “known”, and “meant”. Of these four words, two are *mouth leading* (i.e., mouth movements start before speech sounds) and two are *voice leading* (i.e., sounds start before mouth movements). The experimental finding was that mouth-leading words show a reduced brain response to audiovisual words compared to auditory-only words (Karas et al., 2019). We therefore focus our application to the subset of mouth-leading

words (“last” and “drive”). The data contain 7 subjects with around 64 trials lasting for 3 seconds per subject and a total of 58 Superior Temporal Gyrus (STG) electrodes.

Data preprocessing. The original analog traces are measured at 2000 Hz. We apply notch filters to remove line noise and its harmonics (60, 120 and 180 Hz, etc.). Then a common average reference is used to remove common shifts introduced by patient activities. High-gamma oscillations usually stay above 70 Hz; hence, we apply wavelet transform to extract 70 - 150 Hz activities from the raw analogue traces. The transformed data is further down-sampled to 100 Hz for storage purposes. Each session is sliced into trials according to epoch information. All the trials are aligned to auditory onset, i.e., the time when audio stimuli started to emerge. Because there might be visual information before audio onset for mouth leading words, we collect three seconds of data for each trial, with one second prior and two seconds poster to audio onset. Since brain activity levels often shift for each trial and frequency, we calibrate the signals of high-gamma activities against their own baselines (the average signals during the baseline period from -1 to -0.3 seconds). After the baseline period, we collapse the data by frequencies, resulting in a 301 time-point functional data for each trial and electrode.

The functional response Y is an 64×301 matrix. The design matrix X is 64×2 , with the first column being constant one for the intercept and the second column indicating whether visual stimuli are present. The second regression coefficient $\beta_2(t)$ reflects the effect of audiovisual (AV) stimuli versus auditory only (A) stimuli, and is of primary interest in this study. The time domain \mathcal{T} is partitioned into four parts: $\mathcal{T}^1 = [-1, -0.3)$ as the baseline period, $\mathcal{T}^2 = [-0.3, 0)$ containing video onset but without audio in, $\mathcal{T}^3 = [0, 1.5)$ when both auditory and visual stimulus are present, and $\mathcal{T}^4 = [1.5, 2]$ as clip offset. Since each trial is calibrated to the baseline, the only difference prior and post to onset is the experimental stimuli. Hence, the regression coefficient $\beta_2(t)$ is zero during the baseline period, and non-zero when experiment stimuli present and exhibit effects. Consequently, the estimation of the locally sparse function $\beta_2(t)$ as well as detection of its support is of particular interest.

We use $K = 50$ when implementing the proposed method and select λ and α by the adjusted EBIC. Figure 6 plots the fitted coefficients for $\beta_2(t)$, AV versus A effect. In the proposed weighted functional group bridge approach, we do observe no significant signals in baseline window, while the other methods deviate from this expectation. According to Karas et al. (2019), we should expect a negative AV-A response after auditory onset. Because the proposed functional group bridge method is sparse on non-significant responses, it becomes easy not only to observe the suppression ($AV < A$), but to locate the starting time of that suppression as well as to automate the detection of duration of significant AV versus A effect.

With the evidence that visual stimuli may suppress activities for words “drive” and “last”, we further explore which brain areas have the AV less than A-only response present. Figure 7 visualize all electrodes based on the N27 template brain (Holmes et al., 1998), and we focus on posterior STG electrodes. The average response within 500 ms after auditory onset indicates that p-STG activities are suppressed by additional visual stimuli when audio is present. To test the significance, we further calculate p-values for each electrodes under the null hypothesis that there is no suppression ($AV \geq A$). The z-score is derived from $\min_t \{\hat{\beta}(t)/\hat{\sigma}(t)\}$, the minimum fitted coefficients element-wisely divided by joint standard deviation. Visualizing the p-values, we find p-STG area is highly significant on all subjects involved in the experiment. This evidence for cross-modal suppression of auditory

High-Gamma Response: AV – A

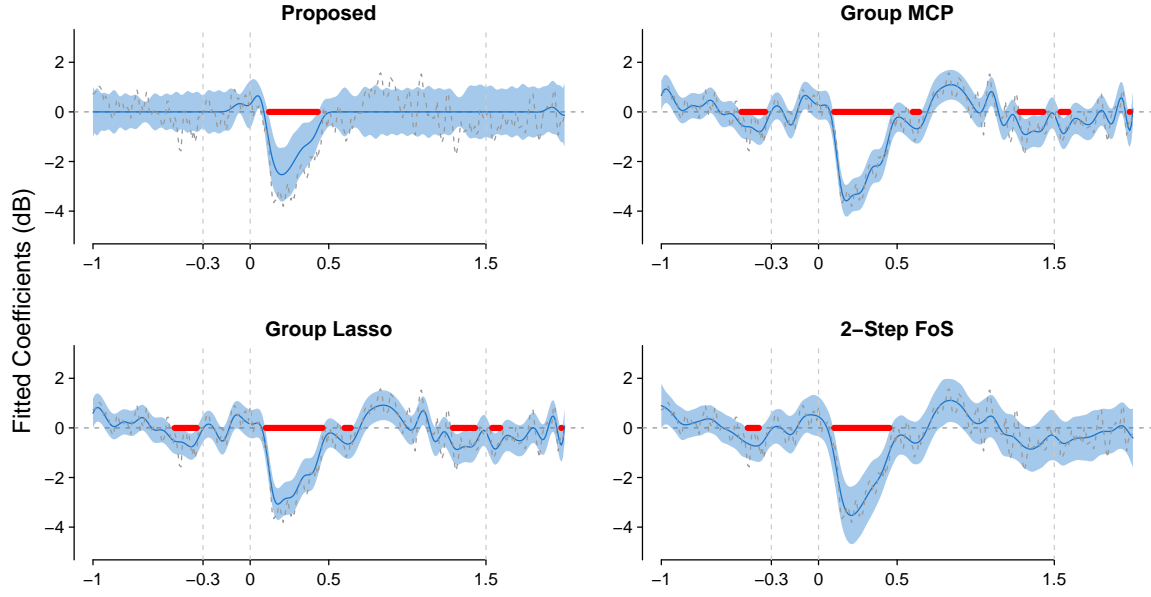


Figure 6: Fitted responses between AV condition versus A-only are colored in blue, solid lines. The light-blue ribbons are the joint 95% CI. Grey dash-lines are the results from OLS fitted coefficients.

cortex complements the previous work (Ozker et al., 2018) and (Karas et al., 2019), showing that multisensory interactions are a powerful modulator of activity throughout the speech perception network.

6 Proofs

In this section, we prove all theorems in the main paper. We begin with two simple lemmas related to B-splines that will be used in the subsequent proofs.

Lemma 6.1. *Suppose Assumptions 5 and 6 hold and the B-spline order satisfies $q \geq 4$. Then for all $v \in \mathbb{R}^K$ such that $\|v\|_2 = 1$, we have*

$$\left\| \sum_{k=1}^K v_k \phi_k(t) \right\|_2^2 \asymp K^{-1}, \quad \frac{K}{T} v^T B B^T v \asymp 1.$$

Proof of Lemma 6.1. Let D be the diagonal matrix whose k^{th} diagonal element is $(t_{m_k+q} - t_{m_k})/q$, where q is the order of B-splines. According to Theorem 5.2 in De Boor (1976), there exists a constant C_q that only depends on q such that

$$C_q^{-1} \|D^{1/2} v\|_2 \leq \left\| \sum_{k=1}^K v_k \phi_k(t) \right\|_2 \leq \|D^{1/2} v\|_2,$$

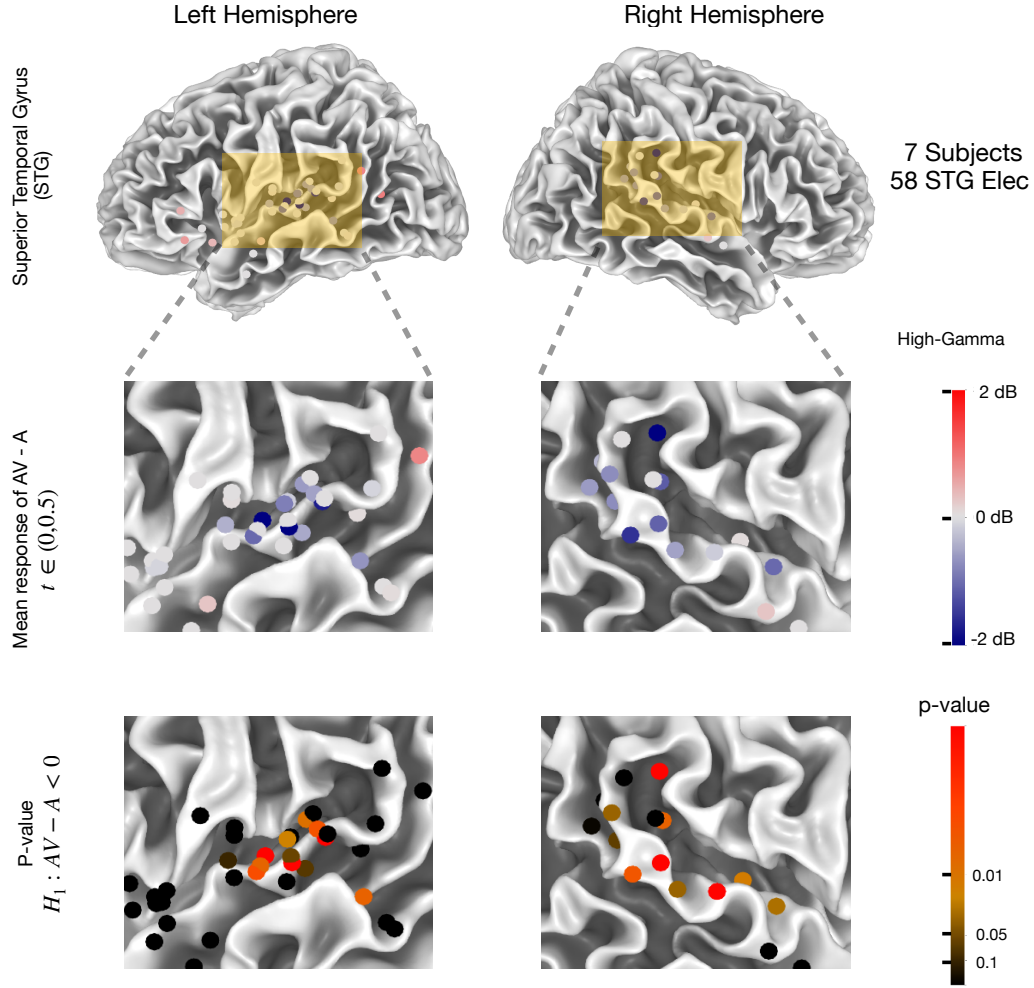


Figure 7: **First row:** position of all 58 electrodes mapped onto N27 brain. **Second row:** mean response of AV-A from auditory onset to 500 ms after onset. Blue electrodes suggest suppression introduced by visual stimuli. Electrodes rendered in gray shows little to no differences, and red electrodes means AV is greater than A. **Third row:** p-values for each electrodes with alternative hypothesis of AV less than A response.

which leads to $\left\| \sum_{k=1}^K v_k \phi_k(t) \right\|_2^2 \asymp K^{-1} \|v\|_2^2 = K^{-1}$ under Assumption 6 that $t_{m_{k+q}} - t_{m_k} \asymp K^{-1}$.

Because B-splines are continuously differentiable of order $q - 2$, $\left\| \sum_{k=1}^K v_k \phi_k(t) \right\|_2^2$ can be approximated by its Riemann sum:

$$\left\| \sum_{k=1}^K v_k \phi_k(t) \right\|_2^2 = \frac{1}{T} \|v^T B\|_2^2 + O \left[\max_m (t_{m+1} - t_m)^{q-2} \right] = \frac{1}{T} \|v^T B\|_2^2 + O(T^{-q+2}).$$

With $K < T$ and $q \geq 4$, we have

$$\frac{K}{T} v^T B B^T v = K \left\| \sum_{k=1}^K v_k \phi_k(t) \right\|_2^2 + O(KT^{-q+2}) \asymp \|v\|_2^2 + O(K^{-q+3}) \asymp 1.$$

□

Lemma 6.2. *For any $\beta_j^*(t)$ satisfying Assumption 1 and 6, let $\tilde{\beta}_j^*(t) = \sum_{k=1}^K \tilde{\gamma}_{jk}^* \phi_k(t)$ be the B-spline approximation proposed by Schumaker (2007) such that $\|\tilde{\beta}_j^*(t) - \beta_j^*(t)\|_\infty \leq C_{\beta_j}^* K^{-r}$ for a constant $C_{\beta_j}^*$. Then there exists a sparse modification $\tilde{\beta}_j(t) := \sum_{k=1}^K \tilde{\gamma}_{jk} \phi_k(t)$ and a constant C_{β_j} such that $S(\beta_j^*(t)) \subseteq S(\tilde{\beta}_j(t))$, and $\|\beta_j^*(t) - \tilde{\beta}_j(t)\|_\infty \leq C_{\beta_j} K^{-r}$. Also for any $t \notin S(\tilde{\beta}_j(t))$, $\sum_{k: \phi_k(t) > 0} |\tilde{\gamma}_{jk}| \geq \frac{C_{\beta_j}^*}{q C_{\beta_j} + C_{\beta_j}^*} |\beta_j^*(t)|$.*

Proof of Lemma 6.2. We first consider a B-spline approximation by shrinking $\tilde{\gamma}_{jk}^*$ such that $|\tilde{\gamma}_{jk}^*| < \frac{C_{\beta_j}^*}{q} K^{-r}$ to zero. Define $\tilde{\gamma}_{jk}^{**} := \tilde{\gamma}_{jk}^* I(|\tilde{\gamma}_{jk}^*| < \frac{C_{\beta_j}^*}{q} K^{-r})$ and $\tilde{\beta}_j^{**} := \sum_{k=1}^K \tilde{\gamma}_{jk}^{**} \phi_k(t)$ as the induced approximation. This new B-spline approximation satisfies that

$$\|\tilde{\beta}_j^{**}(t) - \beta_j^*(t)\|_\infty \leq \|\tilde{\beta}_j^*(t) - \beta_j^*(t)\|_\infty + \sum_{k: |\tilde{\gamma}_{jk}^*| < C_{\beta_j}^* K^{-r}/q} |\tilde{\gamma}_{jk}^*| \phi_k(t) \leq 2C_{\beta_j}^* K^{-r}.$$

Next, we partition B-spline knots as follows,

$$\begin{aligned} A_j^1 &:= A_j^1(\beta_j^*) = \left\{ k : \exists t \in [t_{m_k}, t_{m_{k+1}}] \text{ such that } |\beta_j^*(t)| < C_{\beta_j}^* K^{-r} \right\} \\ A_j^2 &:= A_j^2(\beta_j^*) = \{ k : k < k' \leq k + q, k' \in A_j^1 \} \\ A_j^3 &:= A_j^3(\beta_j^*) = \{ k : k \notin A_j^1 \cup A_j^2 \}. \end{aligned}$$

Let $S_j^z := \{t : t \in [t_{m_k}, t_{m_{k+1}}], k \in A_j^z\}$ for $z = 1, 2, 3$, then it is easy to show $S(\beta_j) \subseteq S_j^1$. Also, for any $t \in [t_{m_k}, t_{m_{k+1}}] \subseteq S_j^1$, there exists at least one $t' \in [t_{m_k}, t_{m_{k+1}}]$ such that $|\beta_j^*(t')| < C_{\beta_j}^* K^{-r}$. By the triangle inequality and $\max_k (t_{m_{k+1}} - t_{m_k}) \leq C_6 K^{-1}$ as in Assumption 6,

$$|\tilde{\beta}_j^*(t)| \leq |\tilde{\beta}_j^{**}(t) - \beta_j^*(t)| + |\beta_j^*(t')| + |\beta_j^*(t) - \beta_j^*(t')| \leq [3C_{\beta_j}^* + L_{\beta_j}^* C_6^r] K^{-r}. \quad (11)$$

We define refined sparse modifications $\tilde{\gamma}$ and $\tilde{\beta}_j(t)$ by

$$\tilde{\gamma}_{jk} = \tilde{\gamma}_{jk}^{**} I\{k \in A_j^3\}, \quad \tilde{\beta}_j(t) = \sum_{k=1}^K \tilde{\gamma}_{jk} \phi_k(t).$$

Such $\tilde{\beta}_j(t)$'s preserve the sparsity of $\beta^*(t)$. In particular, we have $\{k : \phi_k(t) > 0, t \in S_j^1\} \subseteq A_j^1 \cup A_j^2$ according to construction of B-splines, which implies $\tilde{\beta}_j(t) = 0$ for any $t \in S_j^1$, i.e., $S(\beta_j^*) \subseteq S(\tilde{\beta}_j)$. In addition, we can show that $\|\beta_j^*(t) - \tilde{\beta}_j(t)\|_\infty \leq C_{\beta_j} K^{-r}$ for some constant C_{β_j} . To see this, we first note that

$$|\beta_j^*(t) - \tilde{\beta}_j(t)| \leq |\beta_j^*(t) - \tilde{\beta}_j^{**}(t)| + |\tilde{\beta}_j^{**}(t) - \tilde{\beta}_j(t)| \leq 2C_{\beta_j}^* K^{-r} + \max_k |\tilde{\gamma}_{jk}^{**} - \tilde{\gamma}_{jk}|,$$

where we used $|\tilde{\beta}_j^{**}(t) - \tilde{\beta}_j(t)| \leq \max_k |\tilde{\gamma}_{jk}^{**} - \tilde{\gamma}_{jk}| \sum_{k=1}^K \phi_k(t)$. For any k such that $\tilde{\gamma}_{jk}^{**} \neq \tilde{\gamma}_{jk}$, by construction we have $k \in A_j^1 \cup A_j^2$. Thus, there always exists at least one $k' \in A_j^1$ such that $k \leq k' \leq k + q$. According to (11), $|\tilde{\beta}_j^{**}(t')| \leq [3C_{\beta_j}^* + L_{\beta_j}^* C_6^r] K^{-r}$ for any $t' \in [t_{m_{k'}}, t_{m_{k'+1}}]$. By the local support property of B-splines, there are at most q B-splines that are non-zero at t' , and particularly $\tilde{\gamma}_{jk}^{**} \phi_k$ is one of them. In view of Theorem 5.2 in De Boor (1976), $|\tilde{\gamma}_{jk}^{**}|$ is upper bounded by $[3C_{\beta_j}^* + L_{\beta_j}^* C_6^r] K^{-r}$ up to a constant. Therefore, there exists a constant C_{β_j} such that $\|\beta_j^*(t) - \tilde{\beta}_j(t)\|_\infty \leq C_{\beta_j} K^{-r}$.

Finally, for all $t \notin S(\tilde{\beta}_j(t))$, there exists at least one k such that $\tilde{\gamma}_{jk} \neq 0$ and $\phi_k(t) > 0$. In this case, $|\tilde{\gamma}_{jk}| = |\tilde{\gamma}_{jk}^{**}| \geq C_{\beta_j}^* K^{-r}/q$. Hence,

$$\frac{\sum_{k:\phi_k(t)>0} |\tilde{\gamma}_{jk}|}{|\beta_j^*(t)|} \geq \frac{\sum_{k:\phi_k(t)>0} |\tilde{\gamma}_{jk}|}{|\beta_j^*(t) - \tilde{\beta}_j(t)| + |\tilde{\beta}_j(t)|} \geq \frac{\sum_{k:\phi_k(t)>0} |\tilde{\gamma}_{jk}|}{C_{\beta_j} K^{-r} + \sum_{k:\phi_k(t)>0} |\tilde{\gamma}_{jk}|} \geq \frac{C_{\beta_j}^*}{qC_{\beta_j} + C_{\beta_j}^*}.$$

This completes the proof. \square

Proof of Theorem 3.1. Denote $a_{n,\kappa} := n^{\frac{\kappa}{4r} - \frac{c_\kappa}{2}}$, and let $\tilde{\gamma}$ be the sparse modified B-spline coefficients defined in Lemma 6.2. In order to prove $\|\hat{\gamma} - \tilde{\gamma}\|_2 = O_p(a_{n,\kappa})$, it is sufficient to show that, for arbitrary small $\epsilon > 0$, there exists a universal constant C such that

$$P\left\{\inf_{\|u\|_2=C} L(\tilde{\gamma} + a_{n,\kappa}u) > L(\tilde{\gamma})\right\} > 1 - \epsilon, \quad (12)$$

for all sufficiently large n .

Write $L(\tilde{\gamma} + a_{n,\kappa}u) - L(\tilde{\gamma})$ into

$$L(\tilde{\gamma} + a_{n,\kappa}u) - L(\tilde{\gamma}) = [f(\tilde{\gamma} + a_{n,\kappa}u) - f(\tilde{\gamma})] + \lambda[g(\tilde{\gamma} + a_{n,\kappa}u) - g(\tilde{\gamma})]. \quad (13)$$

We next bound the two terms on the right of (13) for all u such that $\|u\|_2 = C$, where C is to be determined later.

Lower bound of $f(\tilde{\gamma} + a_{n,\kappa}u) - f(\tilde{\gamma})$. For any γ ,

$$2f(\gamma) = \|(Y - X\gamma B)W\|_2^2 = \sum_{i=1}^n \|(X_i^T \gamma B - Y_i^T)W\|_2^2.$$

Hence,

$$\begin{aligned}
2f(\gamma + a_{n,\kappa}u) - 2f(\gamma) &= \sum_{i=1}^n \left\| [X_i^T(\gamma + a_{n,\kappa}u)B - Y_i^T]W \right\|_2^2 - \left\| (X_i^T\gamma B - Y_i^T)W \right\|_2^2 \\
&= \sum_{i=1}^n [X_i^T a_{n,\kappa}uB + 2X_i^T\gamma B - 2Y_i^T]WW^T[a_{n,\kappa}X_i^T uB]^T \\
&= a_{n,\kappa}^2 \sum_{i=1}^n X_i^T uBWW^T B^T u^T X_i + 2a_{n,\kappa} \sum_{i=1}^n (X_i^T\gamma B - Y_i^T)WW^T B^T u^T X_i. \tag{14}
\end{aligned}$$

Since $Y = X\gamma B + \theta + XR + E$, where R is B-spline approximation error, we have $X_i^T\gamma B - Y_i^T = -X_i^T R - E_i^T - \theta_i$. Substituting this representation into (14) and letting $\gamma = \tilde{\gamma}$ yields

$$\begin{aligned}
2f(\tilde{\gamma} + a_{n,\kappa}u) - 2f(\tilde{\gamma}) &= a_{n,\kappa}^2 \sum_{i=1}^n X_i^T uBWW^T B^T u^T X_i \\
&\quad - 2a_{n,\kappa} \sum_{i=1}^n X_i^T RWW^T B^T u^T X_i \\
&\quad - 2a_{n,\kappa} \sum_{i=1}^n (E_i + \theta_i)^T WW^T B^T u^T X_i =: I_1 - 2I_2 - 2I_3. \tag{15}
\end{aligned}$$

The first term I_1 in (15) can be bounded below by

$$\begin{aligned}
I_1 &\geq a_{n,\kappa}^2 \frac{nT}{K} \delta_{\min}(WW^T) \delta_{\min}\left(\frac{K}{T}BB^T\right) \frac{1}{n} \sum_{i=1}^n \|X_i^T u\|_2^2 \\
&\geq a_{n,\kappa}^2 \frac{nT}{K} \delta_{\min}(WW^T) \delta_{\min}\left(\frac{K}{T}BB^T\right) \sum_{i=1}^n \delta_{\min}\left(\frac{X^T X}{n}\right) C^2, \tag{16}
\end{aligned}$$

where the last step follows from

$$\sum_{i=1}^n \|X_i^T u\|_2^2 = \|X^T u\|_2^2 = \sum_{k=1}^K \|Xu_k\|_2^2 \geq \delta_{\min}(X^T X) \sum_{k=1}^K \|u_k\|_2^2 = n\delta_{\min}(X^T X/n) C^2.$$

We now substitute the eigenvalue conditions in Assumption 4 and Lemma 6.1 into (16) to obtain that

$$I_1 \geq C_0 a_{n,\kappa}^2 \frac{nT}{K} C^2 = C_0 a_{n,\kappa}^2 n^{1+\frac{\tau-\kappa}{2r}}, \tag{17}$$

for some constant $C_0 > 0$ when n is sufficiently large.

We bound the second term I_2 in (15) by

$$\begin{aligned}
I_2 &= a_{n,\kappa} \sum_{i=1}^n X_i^T R W W^T B^T u^T X_i \leq a_{n,\kappa} \sum_{i=1}^n \|X_i^T\|_2 \|R W W^T B^T\|_2 \|u\|_2 \|X_i\|_2 \\
&= a_{n,\kappa} \sum_{i=1}^n X_i^T X_i C \|R\|_2 \|W W^T\|_2 \|B^T\|_2 \\
&\leq a_{n,\kappa} n \delta_{\max} \left(\frac{X^T X}{n} \right) \delta_{\max}(W W^T) \|R\|_2 \|B\|_2 C \\
&= a_{n,\kappa} O \left(\frac{nT}{\sqrt{K}} K^{-r} \right) C = O \left(a_{n,\kappa}^2 n^{1+\frac{\tau-\kappa}{2r}} \right), \tag{18}
\end{aligned}$$

where (18) is obtained by noticing $\|R\|_2 = O(R^{-r} T^{1/2})$, $K^{-r+1/2} \leq a_{n,\kappa}$ by the definition of $a_{n,\kappa}$, and $\|B\|_2^2 \asymp T/K$ by Lemma 6.1.

For the third term I_3 in (15), we apply the Cauchy-Schwarz inequality to obtain

$$\begin{aligned}
\sum_{i=1}^n (E_i + \theta_i)^T W W^T B^T u^T X_i &= O_p \left[\delta_{\max}(B W W^T) \sqrt{\text{cov} \left(\sum_{i=1}^n \sum_{t=1}^T (E_{it}^2 + \theta_{it}^2) \right)} \right] C \\
&= O_p \left(\sqrt{TK^{-1}} \sqrt{nT} \sqrt{\text{cov}(E_{11}^2 + \theta_{11}^2)} \right) C = O_p \left(n^{1+\frac{\tau-\kappa}{2r}} \sqrt{\text{cov}(E_{11}^2 + \theta_{11}^2)} \right) C.
\end{aligned}$$

According to the sub-Gaussianity condition in Assumption 3, we have $\text{cov}(E_{11}^2 + \theta_{11}^2) = O_p(1)$. Therefore,

$$I_3 = a_{n,\kappa} \sum_{i=1}^n (E_i + \theta_i)^T W W^T B^T u^T X_i = O_p \left(a_{n,\kappa}^2 n^{1+\frac{\tau-\kappa}{2r}} \right) C. \tag{19}$$

Combining (17), (18), and (19), we derive the following lower bound

$$f(\tilde{\gamma} + a_{n,\kappa} u) - f(\tilde{\gamma}) \geq a_{n,\kappa}^2 n^{1+\frac{\tau-\kappa}{2r}} \left[\frac{C_0}{2} C^2 - O(1)C - O_p(1)C \right]. \tag{20}$$

Lower bound of $\lambda[g(\tilde{\gamma} + a_{n,\kappa} u) - g\tilde{\gamma}]$. We first bound $g_{j,m}(\tilde{\gamma} + a_{n,\kappa} u) - g_{j,m}(\tilde{\gamma})$ by considering two cases as follows. If $\|\mathbf{1}(B^{(m)}) \odot \tilde{\gamma}_j\|_1 > a_{n,\kappa} \|\mathbf{1}(B^{(m)}) \odot u_j\|_1$, in view of the inequality $|y^\alpha - x^\alpha| = |y^{\alpha-1} \cdot y - x^{\alpha-1} \cdot x| \leq x^{\alpha-1} |y - x|$ for any $x, y > 0$ and $\alpha \in (0, 1]$, we obtain that

$$\begin{aligned}
&|g_{j,m}(\tilde{\gamma} + a_{n,\kappa} u) - g_{j,m}(\tilde{\gamma})| \\
&\leq \|\mathbf{1}(B^{(m)}) \odot \tilde{\gamma}_j\|_1^{\alpha-1} \left| \|\mathbf{1}(B^{(m)}) \odot (\tilde{\gamma} + a_{n,\kappa} u)_j\|_1 - \|\mathbf{1}(B^{(m)}) \odot \tilde{\gamma}_j\|_1 \right| \\
&\leq \|\mathbf{1}(B^{(m)}) \odot \tilde{\gamma}_j\|_1^{\alpha-1} a_{n,\kappa} \|\mathbf{1}(B^{(m)}) \odot u_j\|_1.
\end{aligned}$$

If $0 < \|\mathbf{1}(B^{(m)}) \odot \tilde{\gamma}_j\|_1 \leq a_{n,\kappa} \|\mathbf{1}(B^{(m)}) \odot u_j\|_1$, then

$$g_{j,m}(\tilde{\gamma} + a_{n,\kappa} u) - g_{j,m}(\tilde{\gamma}) \geq -g_{j,m}(\tilde{\gamma}) \geq -\|\mathbf{1}(B^{(m)}) \odot \tilde{\gamma}_j\|_1^{\alpha-1} a_{n,\kappa} \|\mathbf{1}(B^{(m)}) \odot u_j\|_1.$$

Therefore, in both cases there holds

$$g_{j,m}(\tilde{\gamma} + a_{n,\kappa}u) - g_{j,m} \geq -a_{n,\kappa} \|\mathbf{1}(B^{(m)}) \odot \tilde{\gamma}_j\|_1^{\alpha-1} \|\mathbf{1}(B^{(m)}) \odot u_j\|_1.$$

According to Lemma 6.2, either $\|\mathbf{1}(B^{(m)}) \odot \tilde{\gamma}_j\|_1 = 0$ or $\|\mathbf{1}(B^{(m)}) \odot \tilde{\gamma}_j\|_1 \geq C_1 |\beta_j^*(t)|$ for some constant C_1 . As a result,

$$\begin{aligned} & \lambda \sum_{j,m} g_{j,m}(\tilde{\gamma} + a_{n,\kappa}u) - g_{j,m}(\tilde{\gamma}) \\ & \geq -\lambda a_{n,\kappa} \sum_{\substack{j,m \\ |\tilde{\gamma}_j|^{T\mathbf{1}(B^{(m)})} > 0}} \|\mathbf{1}(B^{(m)}) \odot \tilde{\gamma}_j\|_1^{\alpha-1} \|\mathbf{1}(B^{(m)}) \odot u_j\|_1 \\ & \geq -\lambda a_{n,\kappa} \left(\sum_{\substack{j,m \\ |\tilde{\gamma}_j|^{T\mathbf{1}(B^{(m)})} > 0}} \|\mathbf{1}(B^{(m)}) \odot \tilde{\gamma}_j\|_1^{2\alpha-2} \right)^{1/2} \left(\sum_{j,m} \|\mathbf{1}(B^{(m)}) \odot u_j\|_1^2 \right)^{1/2} \\ & \geq -\lambda C_1^{\alpha-1} \left(T \int_{\beta_j^*(t) \neq 0} \beta_j^*(t)^{2\alpha-2} dt \right)^{1/2} q a_{n,\kappa} C \geq -C_2 a_{n,\kappa}^2 n^{1+\frac{\tau-\kappa}{2r}} C^\alpha, \end{aligned} \quad (21)$$

where $C_2 = q \left(\int_{\beta_j^*(t) \neq 0} \beta_j^*(t)^{2\alpha-2} dt \right)^{1/2}$ and the last step in (21) follows the assumption that $\frac{\log(\lambda)}{\log(n)} \leq 1 - \frac{c\kappa}{2} + \frac{\tau}{4r} - \frac{\kappa}{4r}$.

We now substitute (20) and (21) into (13) and obtain that

$$L(\tilde{\gamma} + a_{n,\kappa}u) - L(\tilde{\gamma}) \geq a_{n,\kappa}^2 n^{1+\frac{\tau-\kappa}{2r}} \left[\frac{C_0}{2} C^2 - O_p(1)C - O(1)C^\alpha \right]. \quad (22)$$

Note that the constant C_0 does not depend on n . For arbitrary small $\epsilon > 0$, we can always choose a sufficiently large constant C such that $\frac{C_0}{2} C^2 - O_p(1)C - O(1)C^\alpha > 0$ holds with probability at least $1 - \epsilon$ for sufficiently large n . Since $a_{n,\kappa}^2 n^{1+\frac{\tau-\kappa}{2r}} \geq 1$ for any $n > 0$, the right hand side of (22) is positive with probability at least $1 - \epsilon$, leading to (12). This completes the proof. \square

Proof of Theorem 3.2. We apply the triangle inequality $\|\hat{\beta}_j - \beta_j^*\|_2 \leq \|\hat{\beta}_j - \tilde{\beta}_j\|_2 + \|\tilde{\beta}_j - \beta_j^*\|_2$ to decompose $\|\hat{\beta}_j - \beta_j^*\|_2$ into estimation error and approximation error. For $t \in [0, 1]$, there holds $\|\tilde{\beta}_j - \beta_j^*\|_2 \leq \|\tilde{\beta}_j - \beta_j^*\|_\infty = O(K^{-r})$. Since $K^{-r} = n^{-\frac{\kappa}{2}} \leq n^{-\frac{c\kappa}{2}}$, it suffices to calculate the rate for the dominating estimation error.

In view of Lemma 6.1, we have $\|\hat{\beta}_j - \tilde{\beta}_j\|_2^2 \asymp n^{-\frac{\kappa}{2r}} \|\hat{\gamma}_j - \tilde{\gamma}_j\|_2^2$, which combined with $\|\hat{\gamma} - \tilde{\gamma}\|_2 = O_p(n^{\frac{\kappa}{4r} - \frac{c\kappa}{2}})$ in Theorem 3.1 gives

$$\|\hat{\beta}_j - \tilde{\beta}_j\|_2 \asymp n^{-\frac{\kappa}{4r}} \|\hat{\gamma}_j - \tilde{\gamma}_j\|_2 = O_p(n^{-\frac{c\kappa}{2}}).$$

The L_∞ norm rate is established in a similar manner by noting that

$$\|\hat{\beta}_j - \tilde{\beta}_j\|_\infty \leq \|\hat{\gamma} - \tilde{\gamma}\|_\infty \sum_{k=1}^K \|\phi_k(t)\|_1 \leq \|\hat{\gamma} - \tilde{\gamma}\|_2 = O_p(n^{\frac{\kappa}{4r} - \frac{c\kappa}{2}})$$

as $\sum_{k=1}^K \phi_k(t) = 1$. This completes the proof. \square

Proof of Theorem 3.3. For each $\beta_j^*(t)$, we apply the same partition to B-spline knots as in Lemma 6.2 and define another sparse modification of the estimator $\hat{\gamma}'$ by $\hat{\gamma}'_{jk} = \hat{\gamma}_{jk} I\{k \in A_j^3\}$. Similar to the argument in Lemma 6.2, we can easily show that $\hat{\beta}'(t) = 0$ when $t \in S_j^1$.

According to the KKT condition (2.3), there holds $\frac{\partial}{\partial \gamma_j} f(\hat{\gamma}) + \sum_{j=1}^p \lambda \frac{\partial}{\partial \gamma_j} s_{j,m}(\hat{\gamma}, \hat{\zeta}) = 0$ for $j = 1, \dots, p$. Expanding this derivative yields

$$X_j^T (Y - X\hat{\gamma}B) WW^T B^T = \alpha\lambda \sum_{m=1}^T \|\mathbf{1}(B^{(m)}) \odot \hat{\gamma}_j\|_1^{\alpha-1} \left[\mathbf{1}(B^{(m)}) \odot \text{sign}(\hat{\gamma}_j) \right]^T.$$

Because either $\hat{\gamma}_{jk} - \hat{\gamma}'_{jk} = 0$ (when $k \in A_j^3$) or $\hat{\gamma}'_{jk} = 0$ (when $k \notin A_j^3$), we have $(\hat{\gamma}_{jk} - \hat{\gamma}'_{jk})\text{sign}(\hat{\gamma}_{jk}) = |\hat{\gamma}_{jk}| I\{k \notin A_j^3\}$. In addition, $|\hat{\gamma}'_{jk}| \leq |\hat{\gamma}_{jk}|$ results in $\|\mathbf{1}(B^{(m)}) \odot \hat{\gamma}'_j\|_1 \leq \|\mathbf{1}(B^{(m)}) \odot \hat{\gamma}_j\|_1$. Therefore,

$$\begin{aligned} & X_j^T (Y - X\hat{\gamma}B) WW^T B^T (\hat{\gamma}_j - \hat{\gamma}'_j) \\ &= \alpha\lambda \sum_{m=1}^T \|\mathbf{1}(B^{(m)}) \odot \hat{\gamma}_j\|_1^{\alpha-1} \times \sum_{k=1}^K \mathbf{1}(B_k^{(m)}) |\hat{\gamma}_{jk}| I\{k \notin A_j^3\} \\ &= \alpha\lambda \sum_{m=1}^T \|\mathbf{1}(B^{(m)}) \odot \hat{\gamma}_j\|_1^{\alpha-1} [\|\mathbf{1}(B^{(m)}) \odot \hat{\gamma}_j\|_1 - \|\mathbf{1}(B^{(m)}) \odot \hat{\gamma}'_j\|_1] \\ &= \alpha\lambda \sum_{m=1}^T \|\mathbf{1}(B^{(m)}) \odot \hat{\gamma}_j\|_1^\alpha - \alpha\lambda \sum_{m=1}^T \|\mathbf{1}(B^{(m)}) \odot \hat{\gamma}_j\|_1^{\alpha-1} \|\mathbf{1}(B^{(m)}) \odot \hat{\gamma}'_j\|_1 \\ &\leq \alpha\lambda \sum_{m=1}^T [g_{j,m}(\hat{\gamma}) - g_{j,m}(\hat{\gamma}')] = \alpha\lambda \sum_{m:t_m \notin S_j^1} [g_{j,m}(\hat{\gamma}) - g_{j,m}(\hat{\gamma}')] + \alpha\lambda \sum_{m:t_m \in S_j^1} g_{j,m}(\hat{\gamma}) \\ &\leq \lambda \sum_{m:t_m \notin S_j^1} [g_{j,m}(\hat{\gamma}) - g_{j,m}(\hat{\gamma}')] + \alpha\lambda \sum_{m:t_m \in S_j^1} g_{j,m}(\hat{\gamma}). \end{aligned}$$

As a result,

$$\begin{aligned} & X_j^T (Y - X\hat{\gamma}B) WW^T B^T (\hat{\gamma}_j - \hat{\gamma}'_j) + (1 - \alpha)\lambda \sum_{m:t_m \in S_j^1} \|\mathbf{1}(B^{(m)}) \odot \hat{\gamma}_j\|_1^\alpha \\ &\leq \lambda \sum_{m=1}^T [\|\mathbf{1}(B^{(m)}) \odot \hat{\gamma}_j\|_1^\alpha - \|\mathbf{1}(B^{(m)}) \odot \hat{\gamma}'_j\|_1^\alpha] = \lambda \sum_{m=1}^T g_{j,m}(\hat{\gamma}) - \lambda \sum_{m=1}^T g_{j,m}(\hat{\gamma}'), \end{aligned}$$

and consequently,

$$\begin{aligned} & \sum_{j=1}^p X_j^T (Y - X\hat{\gamma}B) WW^T B^T (\hat{\gamma}_j - \hat{\gamma}'_j) + (1 - \alpha)\lambda \sum_{j=1}^p \sum_{m:t_m \in S_j^1} \|\mathbf{1}(B^{(m)}) \odot \hat{\gamma}_j\|_1^\alpha \\ &\leq \lambda g(\hat{\gamma}) - \lambda g(\hat{\gamma}') \leq f(\hat{\gamma}') - f(\hat{\gamma}) = \frac{1}{2} \|(Y - X\hat{\gamma}'B) W\|_2^2 - \frac{1}{2} \|(Y - X\hat{\gamma}B) W\|_2^2 \\ &= \frac{1}{2} \|X(\hat{\gamma} - \hat{\gamma}') BW\|_2^2 + \sum_{j=1}^p X_j^T (Y - X\hat{\gamma}B) WW^T B^T (\hat{\gamma}_j - \hat{\gamma}'_j), \end{aligned}$$

where the display in the second line uses the fact that $\hat{\gamma}$ minimizes the objective function $L(\gamma) = f(\gamma) + \lambda g(\gamma)$ in (2). It thus follows that

$$\begin{aligned} (1 - \alpha)\lambda \sum_{j=1}^p \sum_{m:t_m \in S_j^1} \|\mathbf{1}(B^{(m)}) \odot \hat{\gamma}_j\|_1^\alpha &\leq \frac{1}{2} \|X(\hat{\gamma} - \hat{\gamma}')BW\|_2^2 \\ &\leq \frac{nT}{K} \delta_{\max} \left(\frac{X^T X}{n} \right) \delta_{\max} \left(\frac{K}{T} BB^T \right) \delta_{\max}(WW^T) \|\hat{\gamma} - \hat{\gamma}'\|_2^2 = C_0 n^{1+\frac{\tau-\kappa}{2r}} \|\hat{\gamma} - \hat{\gamma}'\|_2^2, \end{aligned} \quad (23)$$

by applying the eigen conditions in Assumption 4 and Lemma 6.1. Because $0 < \alpha < 1$, the left hand side of the first line in (23) can be further lower bounded by

$$\sum_{j=1}^p \sum_{m:t_m \in S_j} \|\mathbf{1}(B^{(m)}) \odot \hat{\gamma}_j\|_1^\alpha \geq \left(\sum_{j=1}^p \sum_{m:t_m \in S_j} \|\mathbf{1}(B^{(m)}) \odot \hat{\gamma}_j\|_1 \right)^\alpha \geq \|\hat{\gamma} - \hat{\gamma}'\|_1^\alpha. \quad (24)$$

Suppose $\|\hat{\gamma} - \hat{\gamma}'\|_2 > 0$, then combining (23) and (24) gives $(1 - \alpha)\lambda \lesssim n^{1+\frac{\tau-\kappa}{2r}} \|\hat{\gamma} - \hat{\gamma}'\|_2^{2-\alpha}$. Hence

$$P(\|\hat{\gamma} - \hat{\gamma}'\|_2 > 0) \leq P\left[(1 - \alpha)\lambda \leq C_0 n^{1+\frac{\tau-\kappa}{2r}} \|\hat{\gamma} - \hat{\gamma}'\|_2^{2-\alpha}\right]. \quad (25)$$

Noting that $\hat{\gamma}'_{jk} = \tilde{\gamma}_{jk} = 0$ for $k \notin A_j^3$ and $\hat{\gamma}'_{jk} = \hat{\gamma}_{jk}$ for $k \in A_j^3$, we obtain

$$\begin{aligned} \|\hat{\gamma} - \hat{\gamma}'\|_2^2 &= \sum_{j=1}^p \left[\sum_{k \notin A_j^3} \|\hat{\gamma}_{jk} - \hat{\gamma}'_{jk}\|_2^2 + \sum_{k \in A_j^3} \|\hat{\gamma}_{jk} - \hat{\gamma}'_{jk}\|_2^2 \right] \\ &= \sum_{j=1}^p \sum_{k \notin A_j^3} \|\hat{\gamma}_{jk} - \hat{\gamma}'_{jk}\|_2^2 = \sum_{j=1}^p \sum_{k \notin A_j^3} \|\hat{\gamma}_{jk} - \tilde{\gamma}_{jk}\|_2^2 \leq \|\hat{\gamma} - \tilde{\gamma}\|_2^2 = O_p(n^{\frac{\kappa}{4r} - \frac{c\kappa}{2}})^2. \end{aligned}$$

Substituting $\|\hat{\gamma} - \hat{\gamma}'\|_2 = O_p(n^{\frac{\kappa}{4r} - \frac{c\kappa}{2}})$ into the right hand side of (25), we have

$$P(\|\hat{\gamma} - \hat{\gamma}'\|_2 > 0) \leq P\left[\lambda \leq O_p(n^{1+\frac{c\kappa(\alpha-2)}{2} + \frac{\tau}{2r} - \frac{\kappa\alpha}{4r}})\right].$$

According to condition $\lambda \gtrsim n^{1+\frac{c\kappa(\alpha-2)}{2} + \frac{\tau}{2r} - \frac{\kappa\alpha}{4r}}$, one has $P(\|\hat{\gamma} - \hat{\gamma}'\|_2 > 0) \rightarrow 0$. As a result,

$$P\{S(\beta_j^*) \subset S(\hat{\beta}_j)\} \rightarrow 1,$$

as n and T go to infinity. This completes the proof. \square

References

- Abraham, C. and Khadraoui, K. (2015). Bayesian regression with b-splines under combinations of shape constraints and smoothness properties. *Statistica Neerlandica*, 69(2):150–170.
- Barber, R. F., Reimherr, M., and Schill, T. (2017). The function-on-scalar lasso with applications to longitudinal gwas. *Electronic Journal of Statistics*, 11(1):1351–1389.

- Boyd, S., Parikh, N., Chu, E., Peleato, B., and Eckstein, J. (2011). Distributed optimization and statistical learning via the alternating direction method of multipliers. *Foundations and Trends in Machine Learning*, 3:1–122.
- Cai, T. T. and Yuan, M. (2011). Optimal estimation of the mean function based on discretely sampled functional data: Phase transition. *Annals of Statistics*, 39(5):2330–2355.
- Candes, E. and Tao, T. (2007). The dantzig selector: Statistical estimation when p is much larger than n . *Annals of Statistics*, 35(6):2313–2351.
- Chen, J. and Chen, Z. (2008). Extended bayesian information criteria for model selection with large model spaces. *Biometrika*, 95(3):759–771.
- Chen, Y., Goldsmith, J., and Ogden, R. T. (2016). Variable selection in function-on-scalar regression. *Stat*, 5(1):88–101.
- De Boor, C. (1976). Splines as linear combinations of b-splines. a survey. Technical report, Wisconsin University Madison Mathematics Research Center.
- De Boor, C. (1978). *A Practical Guide to Splines*, volume 27. Springer New York.
- Efron, B., Hastie, T., Johnstone, I., and Tibshirani, R. (2004). Least angle regression. *Annals of Statistics*, 32(2):407–499.
- Fan, J. (1993). Local linear regression smoothers and their minimax efficiencies. *Annals of Statistics*, 21:196–216.
- Fan, J. and Li, R. (2001). Variable selection via nonconcave penalized likelihood and its oracle properties. *Journal of the American Statistical Association*, 96(456):1348–1360.
- Fan, J. and Peng, H. (2004). Nonconcave penalized likelihood with a diverging number of parameters. *Annals of Statistics*, 32(3):928–961.
- Fan, J. and Zhang, J.-T. (2000). Two-step estimation of functional linear models with applications to longitudinal data. *Journal of the Royal Statistical Society: Series B (Statistical Methodology)*, 62(2):303–322.
- Fan, Z. and Reimherr, M. (2017). High-dimensional adaptive function-on-scalar regression. *Econometrics and Statistics*, 1:167–183.
- Ferraty, F. and Vieu, P. (2006). *Nonparametric Functional Data analysis: Theory and Practice*. Springer Science & Business Media.
- Fu, W. J. (1998). Penalized regressions: The bridge versus the lasso. *Journal of Computational and Graphical Statistics*, 7:397–416.
- Gunn, L. H. and Dunson, D. B. (2005). A transformation approach for incorporating monotone or unimodal constraints. *Biostatistics*, 6(3):434–449.

- Holmes, C. C. and Heard, N. A. (2003). Generalized monotonic regression using random change points. *Statistics in Medicine*, 22(4):623–638.
- Holmes, C. J., Hoge, R., Collins, L., Woods, R., Toga, A. W., and Evans, A. C. (1998). Enhancement of mr images using registration for signal averaging. *Journal of Computer Assisted Tomography*, 22(2):324–333.
- Huang, J., Horowitz, J. L., and Ma, S. (2008). Asymptotic properties of bridge estimators in sparse high-dimensional regression models. *Annals of Statistics*, 36(2):587–613.
- Huang, J., Horowitz, J. L., and Wei, F. (2010). Variable selection in nonparametric additive models. *Annals of Statistics*, 38(4):2282–2313.
- Huang, J., Ma, S., Xie, H., and Zhang, C.-H. (2009). A group bridge approach for variable selection. *Biometrika*, 96(2):339–355.
- James, G. M., Wang, J., and Zhu, J. (2009). Functional linear regression that’s interpretable. *Annals of Statistics*, 37(5A):2083–2108.
- Karas, P. J., Magnotti, J. F., Metzger, B. A., Zhu, L. L., Smith, K. B., Yoshor, D., and Beauchamp, M. S. (2019). The visual speech head start improves perception and reduces superior temporal cortex responses to auditory speech. *eLife*, 8:e48116.
- Knight, K. and Fu, W. (2000). Asymptotics for lasso-type estimators. *Annals of Statistics*, 28(5):1356–1378.
- Lachaux, J.-P., Axmacher, N., Mormann, F., Halgren, E., and Crone, N. E. (2012). High-frequency neural activity and human cognition: past, present and possible future of intracranial eeg research. *Progress in Neurobiology*, 98(3):279–301.
- Lin, Z., Cao, J., Wang, L., and Wang, H. (2017). Locally sparse estimator for functional linear regression models. *Journal of Computational and Graphical Statistics*, 26(2):306–318.
- Meyer, M. C. (2008). Inference using shape-restricted regression splines. *Annals of Applied Statistics*, 2(3):1013–1033.
- Morris, J. S. (2015). Functional regression. *Annual Review of Statistics and Its Application*, 2(1):321–359.
- Ozker, M., Yoshor, D., and Beauchamp, M. S. (2018). Frontal cortex selects representations of the talker’s mouth to aid in speech perception. *eLife*, 7:e30387.
- Park, C. and Yoon, Y. J. (2011). Bridge regression: Adaptivity and group selection. *Journal of Statistical Planning and Inference*, 141(11):3406–3519.
- Ramsay, J. O. (1998). Estimating smooth monotone functions. *Journal of the Royal Statistical Society: Series B (Statistical Methodology)*, 60(2):365–375.

- Ramsay, J. O. and Silverman, B. W. (2005). *Functional Data Analysis*. Springer New York, 2 edition.
- Schumaker, L. (2007). *Spline Functions: Basic Theory*. Cambridge University Press.
- Shively, T. S., Sager, T. W., and Walker, S. G. (2009). A bayesian approach to non-parametric monotone function estimation. *Journal of the Royal Statistical Society: Series B (Statistical Methodology)*, 71(1):159–175.
- Shively, T. S., Walker, S. G., and Damien, P. (2011). Nonparametric function estimation subject to monotonicity, convexity and other shape constraints. *Journal of Econometrics*, 161:166–181.
- Tibshirani, R. (1996). Regression shrinkage and selection via the lasso. *Journal of the Royal Statistical Society, Series B: Methodological*, 58:267–288.
- Wang, H. and Kai, B. (2015). Functional sparsity: Global versus local. *Statistica Sinica*, pages 1337–1354.
- Wang, J.-L., Chiou, J.-M., and Müller, H.-G. (2016). Functional data analysis. *Annual Review of Statistics and Its Application*, 3:257–295.
- Wang, X. and Wang, M. (2017). Adaptive group bridge estimation for high-dimensional partially linear models. *Journal of Inequalities and Applications*, 2017(1):158.
- Wang, Z., Magnotti, J. F., and Beauchamp, M. S. (2020). Rave: comprehensive open-source software for reproducible analysis and visualization of intracranial eeg data. *bioRxiv*.
- Zhang, C.-H. (2010). Nearly unbiased variable selection under minimax concave penalty. *Annals of Statistics*, 38(2):894–942.
- Zhou, J., Wang, N.-Y., and Wang, N. (2013). Functional linear model with zero-value coefficient function at sub-regions. *Statistica Sinica*, 23(1):25–50.
- Zhu, H., Fan, J., and Kong, L. (2014). Spatially varying coefficient model for neuroimaging data with jump discontinuities. *Journal of the American Statistical Association*, 109(507):1084–1098.
- Zou, H. (2006). The adaptive lasso and its oracle properties. *Journal of the American Statistical Association*, 101(476):1418–1429.
- Zou, H. and Hastie, T. (2005). Regularization and variable selection via the elastic net. *Journal of the Royal Statistical Society: Series B (Statistical Methodology)*, 67(2):301–320.